High-throughput transposon sequencing highlights the cell wall as an important barrier for salt stress in methicillin resistant *Staphylococcus aureus*

Short Title: The global salt stress response in S. aureus

Christopher F. Schuster[a], David M. Wiedemann[a], Freja C. M. Kirsebom[a,1], Marina Santiago[b], Suzanne Walker[b] and Angelika Gründling[a,2]

ORCID IDs: 0000-0002-4566-7226 (CFS), 0000-0001-6961-0980 (DMW), 0000-0003-4585-319X (FCK), 0000-0002-5446-3452 (MS), 0000-0002-0545-914X (SW), 0000-0002-6235-8687 (AG)

[a]Section of Molecular Microbiology and MRC Centre for Molecular Bacteriology and Infection, Imperial College London, London, SW7 2AZ, U.K.

[b]Department of Microbiology and Immunobiology, Harvard Medical School, Boston, MA 02115, U.S.A.

[1]Current address: Section of Respiratory Infections, National Heart and Lung Institute, Imperial College London, London, W2 1PG, U.K.

[2]To whom correspondence should be addressed. Email: a.grundling@imperial.ac.uk, Phone: 0044 20 7594 5256

Keywords: osmotic stress, TN-seq, Tradis, NaCl, *S. aureus*, DUF25380, Pbp2

Summary

Staphylococcus aureus is an opportunistic pathogen that can cause soft tissue infections but is also a frequent cause of foodborne illnesses. One contributing factor for this food association is its high salt tolerance allowing this organism to survive the commonly used food preservation method of salting. How this resistance is mediated is poorly understood, particularly during long-term exposure. In this study, we used TN-seq based screens and identified a number of previously uncharacterized genes that are involved in the salt stress response. Amongst these, we identified the DUF2538 domain containing gene *SAUSA300_0957* (gene *957*) as essential under salt stress. Interestingly, a *957* mutant was less susceptible to oxacillin and showed increased peptidoglycan crosslinking. The salt sensitivity phenotype could be suppressed by amino acid substitutions in the transglycosylase domain of the penicillin binding protein Pbp2, and these changes restored the peptidoglycan crosslinking to WT levels. These results indicate that increased crosslinking of the peptidoglycan polymer can be detrimental and highlight a critical role of the bacterial cell wall for osmotic stress resistance. This study will serve as a starting point for future research on osmotic stress response and help develop better strategies to tackle foodborne staphylococcal infections.

Introduction

Staphylococcus aureus is a Gram-positive bacterium that is carried by about 20 % of healthy individuals (Wertheim *et al.*, 2005). It is also an opportunistic pathogen causing a variety of diseases, including bacteremia, endocarditis, soft tissue infections and food poisoning (Tong *et al.*, 2015). One characteristic of *S. aureus* is its ability to grow in the presence of a very high salt concentration (up to 2.5 M). Many other bacteria are unable to grow under these conditions (Measures, 1975), and this has been used extensively for the isolation of staphylococci. This salt tolerance also allows *S.*

24 *aureus* to thrive in its niches such as the human nares, skin (Wertheim *et al.*, 2005) and certain food
25 products (Adams & Moss, 2008).

26 Bacterial cells are highly pressurized (up to 1.9 MPa for *Bacillus subtilis* (Whatmore & Reed,
27 1990)) and contain a strongly crowded cytoplasm that is hyperosmotic to the environment. Water
28 is not transported into the cell actively but rather influxes passively into the cell due to the high
29 internal osmolality. Whenever the extracellular osmolality increases, water exits the cell which can
30 cause problems to multiple cellular processes, in part due to molecular crowding (Wood, 2011, van
31 den Berg *et al.*, 2017). In the case of salt, an increase in the intracellular sodium concentration can
32 lead to mis- and unfolding of proteins and inhibit enzymatic reactions due to the strong ionic
33 interactions produced. Hence, *S. aureus* must possess strategies to counter the effects of salt
34 damage, but these are poorly understood, as most work has been performed in *Escherichia coli* and
35 *B. subtilis*, which possess much lower salt tolerances than Staphylococci.

36 General mechanisms of hyper-osmotic stress mitigation in bacteria are the rapid import of
37 potassium and the accumulation of small osmotically active compounds, named compatible solutes
38 (reviewed in depth by (Bremer & Krämer, 2019, Gunde-Cimerman *et al.*, 2018, Booth, 2014, Cox *et*
39 *al.*, 2018)). Potassium levels quickly subside in favor of an increase in the concentration of
40 compatible solutes.

41 In *S. aureus,* results consistent with the uptake potassium (Csonka, 1989, Csonka & Hanson,
42 1991, Sleator & Hill, 2002) followed by the accumulation of compatible solutes have been reported
43 (Measures, 1975, Graham & Wilkinson, 1992, Christian & Waltho, 1964). The most effective
44 compatible solutes in *S. aureus* are glycine betaine and proline (Miller *et al.*, 1991, Measures, 1975,
45 Townsend & Wilkinson, 1992, Anderson & Witter, 1982, Bae & Miller, 1992, Pourkomailian & Booth,
46 1992), which are imported by specific osmolyte transporters (Bae & Miller, 1992, Pourkomailian &
47 Booth, 1992). These preferred osmolytes can accumulate in the cell to very high concentrations
48 without negatively affecting cellular processes (Csonka & Hanson, 1991). In addition, *S. aureus* can

49 also synthesize compatible solutes *de novo*, as in the case of glutamine (Anderson & Witter, 1982),
50 but this process is much slower than the uptake of osmolytes and requires more energy.

51 Previous research investigating the underlying genetic factors of the *S. aureus* osmotic stress
52 response implicated several osmolyte transporters in this process (Price-Whelan *et al.*, 2013,
53 Scybert *et al.*, 2003, Schwan *et al.*, 2006, Vijaranakul *et al.*, 1998, Wengender & Miller, 1995). These
54 include the potassium transport systems Kdp and Ktr (Price-Whelan *et al.*, 2013), the proline
55 transporter PutP (Wengender & Miller, 1995, Schwan *et al.*, 2006), the arsenic transport system Ars
56 (Scybert *et al.*, 2003) and the branched chain amino acid uptake system BrnQ (Vijaranakul *et al.*,
57 1998). In addition, although currently not experimentally verified in *S. aureus*, it can be assumed
58 that the main glycine betaine uptake system OpuD (Wetzel *et al.*, 2011, Zeden *et al.*, 2018) is an
59 important factor in *S. aureus* for osmotic adaptation as glycine betaine uptake reduces sensitivity to
60 NaCl exposure (Miller *et al.*, 1991). Of note, in recent time the second messenger cyclic-
61 dinucleotide-AMP (c-di-AMP) (Corrigan & Gründling, 2013) has been tied to the regulation of
62 osmotic stress in *S. aureus* and other Gram-positive bacteria (reviewed by Commichau *et al.*, 2018).
63 This is through the interaction and regulation of a number of potassium (Corrigan *et al.*, 2013) and
64 compatible solute transporters by c-di-AMP (Schuster *et al.*, 2016).

65 Despite these multiple countermeasures, exposure of *S. aureus* to osmotic stress leads to
66 morphological changes, including the formation of larger cells (Vijaranakul *et al.*, 1995) and a
67 thickening of the cell wall (Onyango *et al.*, 2013). However, if and which genetic factors are required
68 for those processes are currently not well understood. The cell wall of Gram-positive bacteria is an
69 important barrier and acts as a counterpart to the pressurized cytoplasm. A major component of
70 the cell wall is peptidoglycan, a polymer consisting of chains of repeating N-acetylglucosamine
71 (GlcNAc) and N-acetylmuramic acid (MurNAc) units that are crosslinked with neighboring chains via
72 short peptides and, in the case of *S. aureus,* pentaglycine cross-bridges (Reviewed by (Vollmer *et al.*,
73 2008)). In the past, the contribution of the cell wall towards osmotic stress resistance was often not

74 considered in the bacterial osmotic stress resistance field. Partly, because the integrity of the cell
75 wall is often assumed to be a prerequisite rather than an active adaptation to survive osmotic
76 stresses and partly because most cell envelope stress sensing systems are unable to directly sense
77 osmotic stresses (Jordan *et al.*, 2008).

78 Nevertheless, several possible changes to the cell wall have been observed *in S. aureus* during
79 NaCl stress, such as shortened interpeptide bridges in the peptidoglycan (Vijaranakul *et al.*, 1995),
80 an increase in resistance to methicillin (Madiraju *et al.*, 1987) and increased autolysis activity
81 (Stapleton *et al.*, 2007, Ochiai, 2000). In addition to peptidoglycan, other components within the cell
82 envelope, such as teichoic acids and more specifically their modifications with D-alanine (Koprivnjak
83 *et al.*, 2006) and sugar residues (Mistretta *et al.*, 2019, Kho & Meredith, 2018) are affected by
84 osmotic stress. Combined, these findings indicate that the integrity of the cell wall is an important
85 requirement for osmotic resistance.

86 Using a transposon insertion sequencing (TN-seq) method (Santiago *et al.*, 2015), we
87 determined on a whole genome level genes that are essential or dispensable during long-term salt
88 exposure. Amongst other novel candidate genes, we identified gene *SAUSA300_0957* as an
89 important salt resistance gene in *S. aureus* and show that the encoded protein is important for
90 peptidoglycan homeostasis in *S. aureus*. Another protein, which we identified as important during
91 salt stress, is the penicillin binding protein Pbp2, further emphasizing a key function of
92 peptidoglycan during NaCl-induced osmotic stress. Taken together, these experiments highlight the
93 bacterial cell wall as a key player in the salt stress response of *S. aureus*.

94 **Results**

95 **TN-seq is a robust method to identify *S. aureus* genes involved in NaCl stress**

96 To identify *S. aureus* genes that are needed during salt stress, we conducted transposon
97 sequencing (TN-seq) screens in the presence and absence of salt (Fig. 1A). These experiments were
98 repeated in two independent TN-seq screens using a previously published library (Santiago *et al.*,
99 2015, Coe *et al.*, 2019) with six transposon variants (Replicate A) and a library containing only one
100 transposon variant (Replicate B) (Supplementary Table S1 for overview). The libraries were
101 propagated for 17 generations in either LBN or LB medium with 0.5 M NaCl and the expected growth
102 reduction was observed in the presence of 0.5 M NaCl (Fig. 1B). The Tn insertions were found to be
103 distributed evenly throughout the genome in the libraries grown in LBN medium. When the libraries
104 were grown in high salt medium, clustering of transposon insertions in certain regions was observed
105 due to the enrichment of better salt-adapted TN-strains (Supplementary Fig. S1). The fold-changes
106 of transposon insertions per gene under the salt stress conditions compared to the LBN condition
107 (input library) as well as q-values were determined for each gene (Supplementary Table S2-S3). The
108 data were plotted as volcano plots (Fig. 1C), revealing similar numbers of conditional salt essential
109 and dispensable genes in both replicates. Furthermore, a good overlap of the top essential and
110 dispensable genes was observed between the replicates confirming the robustness of the TN-Seq
111 screens (Supplementary Tables S3-7).

112 **The TN-seq screens highlight the essentiality of transporters and cell envelope related genes and**
113 **the dispensability of respiration genes under high salt conditions**

114 In both replicates, genes coding for transporters and cell envelope related genes were the most
115 prominent conditionally salt essential genes (Supplementary Tables S4-S7). More specifically, the
116 TN-seq data indicated that inactivation of the putative magnesium transporter MgtE (Schuster *et*

117 *al.*, 2019) and the putative D-serine/D-alanine/glycine transporter AapA is detrimental under salt
118 stress (Supplementary Tables S4 and S6). Inactivation of AapA has previously been shown to
119 suppress the temperature sensitivity phenotype seen in an *S. aureus fmtC/mprF* mutant (Ishibashi
120 *et al.*, 2007) and to lead to increased amoxacillin and daptomycin sensitivity (Mlynek *et al.*, 2016,
121 Coe *et al.*, 2019). In addition, the *dlt* operon, coding for enzymes required for the D-alanylation of
122 teichoic acids, an important factor for cationic peptide resistance (Brown *et al.*, 2013), as well as the
123 stationary and stress sigma factor gene *sigB* were found to be essential.

124 An even larger number of genes was identified as dispensable during salt stress (Supplementary
125 Tables S5 and S7). Inactivating or reducing the expression of such genes is expected to help *S. aureus*
126 survive under salt stress. Among these dispensable genes were genes coding for the sodium
127 antiporter Mnh2, which has previously been shown to transport Na^+/H^+ and K^+/H^+ in high pH
128 medium and to play an important role in cytoplasmic pH maintenance (Vaish *et al.*, 2018). Strikingly,
129 a large number of genes involved in respiration, such as the *cta/qox/men/hem* genes as well as
130 genes involved indirectly in respiration through quinone synthesis (shikimate pathway, *aro* operon)
131 were also identified as dispensable during salt stress. The data also reproducibly indicated that
132 genes coding for the phosphodiesterases GdpP and Pde2 involved in degradation of the signaling
133 molecule c-di-AMP are dispensable under high salt conditions. Using the TN-seq approach, we were
134 able to identify a large number of *S. aureus* genes as potentially dispensable or essential when this
135 organism is exposed to high salt.

136 **Tn-seq reveals previously unidentified salt resistance genes during long-term salt exposure**

137 The TN-seq method relies on the enrichment of strains adapted to certain growth conditions,
138 and is therefore ideal for exploring the long-term effects on growth in response to salt stress. In a
139 previous study (Price-Whelan *et al.*, 2013), the adaptation of *S. aureus* to 2 M NaCl stress after 6
140 generations of growth was determined on a transcriptome level. This work highlighted the

141 importance of K^+ transporters for *S. aureus* to survive the high salt exposure. To evaluate how our
142 results compare, we determined the overlaps between our datasets and the microarray data. To
143 this end, the *S. aureus* strain COL locus tags used in the microarray study were converted to TCH1516
144 locus tags where possible (Supplementary Table S8) and compared to the two TN-seq datasets. The
145 overlap between the downregulated (microarray) and dispensable (TN-seq) genes was minimal in
146 both replicates (1 and 7) and also very small for the upregulated and essential genes (both 14). Three
147 operons were consistently essential or upregulated between all datasets: the *cap5*,
148 *SAUSA300_0771-2*, and the *sda* operon. The *cap5* genes are involved in capsule production (Chan
149 *et al.*, 2014) and this type of capsule has been previously reported to be induced by the addition of
150 salt (Pöhlmann-Dietze *et al.*, 2000). Genes *SAUSA300_0771-2* are hypothetical membrane proteins
151 and presumably part of a threonine/serine exporter (Interpro database IDs: IPR010619 and
152 IPR024528) and the *sda* genes are annotated as L-serine dehydratase components and a regulator
153 protein. The low overlap between the microarray and TN-seq data (Supplementary Table S8)
154 suggests that in our screen we have identified a number of previously unknown salt tolerance genes.

155 **Confirmation of genes essential during salt stress using defined mutants**

156 To determine to what extent different genes identified in the TN-seq screen contribute to the
157 salt resistance of *S. aureus*, a set of potentially salt essential genes from dataset B were chosen for
158 further investigation (Supplementary Table S9). For this analysis we used defined transposon
159 mutants available from the *S. aureus* NTML transposon mutant library (Fey *et al.*, 2013). The growth
160 of the different NTML transposon mutant strains was assessed in LBN and LB 0.5 M NaCl medium.
161 In LBN medium, most strains grew similarly to the WT strain JE2, indicating that inactivation of the
162 respective gene does not greatly affect bacterial growth in normal LB medium (Supplementary Figs.
163 S2A-D, left panels). Exceptions were strains NE1109 (*sigB*), NE1778 (*lcpB*) and NE188 (*mfd*), cultures
164 of which reached slightly lower final optical densities (Supplementary Figs. S2A-D, left panels). At

165 high osmolality conditions (LB 0.5 M NaCl), all strains showed a growth defect compared to the WT
166 strain (Supplementary Figs. S2A-D, right panels), validating the TN-seq as a method to identify *S.*
167 *aureus* genes that are important during salt stress. Several strains exhibited strong growth defects
168 in the presence of 0.5 M NaCl with strain NE1384, containing a transposon insertion in
169 *SAUSA300_0957* showing extremely reduced growth (Supplementary Figs. S2C and D). To confirm
170 that the salt sensitivity was mediated by the inactivation of the genes in questions, we constructed
171 complementation plasmids for seven of the most promising candidates by either expressing the
172 gene of interest from its native promoter or an anhydrotetracycline (Atet) inducible promoter in the
173 transposon mutant strains. While no complementation was observed for four strains
174 (Supplementary Figs. S3A and S3B), the salt-dependent growth defect could be complemented for
175 strains carrying mutations in *SAUSA300_0694* (Fig. 2A), *SAUSA300_0910* (*mgtE*) and
176 *SAUSA300_0957* (Fig. 2B). *SAUSA300_0694* encodes a hypothetical protein with 6 predicted
177 transmembrane helices but no other identifiable domain motif. MgtE (SAUSA300_0910) is a
178 predicted magnesium transporter, which we have recently shown can also contribute to cobalt
179 toxicity in *S. aureus* (Schuster *et al.*, 2019). *SAUSA300_0957* (from here on out referred to as gene
180 *957*) codes for a cytoplasmic protein with a DUF2538 domain of unknown function that is conserved
181 in Actinobacteria and Firmicutes. We further investigated this gene in this study because the *957*
182 mutant exhibited the strongest salt-sensitivity phenotype (Fig. 2B).

183 **Deletion of gene *957* causes physiological changes leading to a smaller cell size**

184 As all previous experiments were performed with transposon mutants, we first constructed
185 strain LAC*Δ*957* with a marker-less in-frame deletion of gene *957*. Strain LAC*Δ*957* had the
186 expected growth defect in the presence of 0.5 M NaCl and this phenotype could be complemented
187 by expressing a functional copy of *957* (Fig. 3A). To gain further insight into the molecular function
188 of gene *957*, we analyzed the neighboring genomic area. Transcriptome data (Mäder *et al.*, 2016)

189 suggested that gene *957* is in an operon with *lcpB* (Fig. 3B), which is one of three wall teichoic acid
190 (WTA) ligases present in *S. aureus* (Chan *et al.*, 2013, Over *et al.*, 2011, Schaefer *et al.*, 2017). *fmtA*
191 is located upstream of *957* and has been proposed to code for an esterase that can remove D-
192 alanine modifications from teichoic acids (Rahman *et al.*, 2016) and is involved in methicillin
193 resistance (Berger-Bächi *et al.*, 1989). Genes coding for a predicted acetyltransferase and *atl* coding
194 for the major *S. aureus* autolysin are found immediately downstream of the *957* operon (Oshida *et*
195 *al.*, 1995). Due to the presence of many cell envelope related genes in the vicinity of gene *957*, we
196 proceeded to test if the *957* mutant displays other phenotypes connected to cell envelope
197 homeostasis. First, WT LAC*, the *957* mutant and the complementation strain were grown in LBN
198 and the ratio of colony forming units to optical density (CFU/OD) was determined. The CFU/OD ratio
199 was significantly larger for the *957* mutant (60.8±6.8 x10^7 CFU/OD) mutant as compared to strain
200 LAC* (37.5±9.3 x10^7 CFU/OD) when grown in LBN, suggesting a change in cell shape or size (Fig. 3C).
201 This phenotype was restored in the complementation strain (37.3±3.6 x10^7 CFU/OD) (Fig. 3C). When
202 the average cell diameter was determined by microscopy, a small but significant reduction in cell
203 diameter was seen for the *957* mutant (1.25±0.02 µm) as compared to the WT (1.36±0.03 µm) and
204 the cell size was restored to wild type levels in the complementation strain (1.35±0.05 nm) (Fig. 3D).
205 These results support our hypothesis that the envelope might be a target of *gene 957* and prompted
206 us to look into these processes in more detail.

207 **Salt sensitivity of *957* is not due to interaction with LcpB but likely due to changes in peptidoglycan**
208 **crosslinking**

209 Since the gene *957* is on the same transcript as *lcpB* coding for a WTA ligase (Fig. 3A), the
210 contribution of WTA to salt stress resistance as well as the contribution of *957* to the attachment of
211 WTA to the cell wall was assessed. Initially the growth of a *tagO* (*tarO/llm*) mutant, a strain unable
212 to produce WTA, was tested in LB and LB 0.5 M NaCl medium. When cells were grown in LBN, they

213 grew normally (Supplementary Fig. S4A), but under high salt conditions, the *tagO* mutant showed
214 reduced growth, similar to that of the *957* mutant (Fig. 4A). This is consistent with what has been
215 reported previously for a *Staphylococcus epidermidis tagO* mutant (Holland *et al.*, 2011) and
216 indicates an important role for WTA during salt stress. When the *lcpB* mutant was propagated in
217 LBN medium, its growth was slightly inhibited (Supplementary Fig. S4A). However, in high salt
218 medium (Fig. 4A) it grew unimpeded and like WT. Since the *lcpB* mutant did not show a growth
219 defect in high salt medium, this made it unlikely that *957* is a regulator of LcpB activity, and hence
220 is involved in the attachment of WTA to the peptidoglycan. To specifically investigate the
221 requirement of 957 in WTA attachment, we isolated WTA from strains grown in either LBN or LB
222 containing 0.4 M NaCl and separated the polymer on native polyacrylamide gels. The slightly lower
223 concentration of salt was chosen because growth of the *957* and the *tagO* mutants was too strongly
224 inhibited at 0.5 M NaCl. As expected the *tagO* mutant did not produce any WTA (Supplementary
225 Fig. S4B, Fig. 4B) and consistent with previous studies (Over *et al.*, 2011, Chan *et al.*, 2013), the *lcpB*
226 mutant exhibited slightly reduced WTA levels compared to the other strains (Supplementary Fig.
227 S4B, Fig. 4B). No reduction in WTA was observable in the *957* mutant compared to the WT strain in
228 either LBN (Supplementary Fig. S4B & S4C) or LB 0.4 M NaCl (Fig. 4B & 4C) but rather a small increase,
229 which could be complemented. Taken together, these data indicate that 957 neither directly nor
230 indirectly (e.g. through regulating the activity of LcpB) plays a major role in WTA attachment.

231 Gene *957* is found upstream of the bi-functional autolysin gene *atl* and therefore we next
232 investigated potential changes in autolytic activity using zymograms. A small increase in autolytic
233 activity was detected in the *957* mutant (Fig. 4D) for bands around 55 kDa and 70 kDa compared to
234 the WT and complementation strain, indicating a possible change in Atl availability. We also tested
235 the susceptibility of the *957* mutant towards the cell wall active beta-lactam antibiotic oxacillin. The
236 *957* mutant exhibited a small but significant increase in MIC towards this antibiotic compared to the
237 WT and the complementation strain (Fig. 4E), indicating potential changes to the peptidoglycan

238 structure. To test this, we next analyzed the muropeptide profile of mutanolysin-digested
239 peptidoglycan isolated from the WT, the *957* mutant and complementation strain after growth in
240 LBN or LB 0.4 M NaCl medium. Upon first inspection, no peaks were absent in any condition or strain
241 (Supplementary Fig. S4D and S4E). Probing further, mono- and multimers of muropeptides up to 7-
242 mers were quantified but no significant changes were found when strains were cultured in LBN
243 medium (Fig. 5A). At the 0.4 M NaCl condition however, the muropeptide profiles of the *957* mutant
244 strain exhibited a significant decrease in the total amount of di- and trimers and a significant
245 increase in higher multimers compared to the WT and complementation strain (Fig. 5B). This
246 underlines the involvement of gene *957* in the cell wall homeostasis and suggests that the sensitivity
247 to NaCl could potentially be caused by higher crosslinking and potentially rigidity of the
248 peptidoglycan in the mutant.

249 **Salt-resistant suppressors possess variations in the transglycosylase domain of Pbp2**

250 Next, we attempted to generate *957* suppressor strains that showed improved growth in the
251 presence of 0.5 M NaCl, with the idea that by mapping and investigating the compensatory
252 mutations, further insight into the cellular functions of protein 957 could be gained. We readily
253 obtained suppressor strains by growth if the *957* mutant strain in NaCl containing liquid medium.
254 These strains grew as well as or even better than the WT LAC* strain in high salt conditions (Fig. 6A)
255 and also grew similar to the WT in LBN (Supplementary Fig. S5A). The genome sequences of 10
256 independent suppressor strains were determined and single nucleotide polymorphisms (SNPs) in
257 one or two genes could be identified for each strain (Supplementary Table S10), except for one
258 strain where the coverage was insufficient, and this strain was omitted from further analysis. A
259 common denominator for all suppressor strains were SNPs in the *pbp2* gene, coding for the Penicillin
260 binding protein 2 (Pbp2) (Fig. 6B). *S. aureus* Pbp2 is a bifunctional enzyme (Wyke, 1984, Murakami
261 *et al.*, 1994), which possesses transglycosylase and transpeptidase activity and is involved in

262 peptidoglycan synthesis. All nine discovered SNPs were unique and led to mutations in the amino
263 acid sequence in the transglycosylase domain but neither to stop codons, nor frameshifts nor
264 mutations in the transpeptidase domain. The mutations were mapped (Fig. 6B) onto an available
265 Pbp2 structure (3DWK) (Lovering *et al.*, 2008) to see if a specific area of the transglycosylase domain
266 had been targeted, but the amino acid substitutions were found throughout the molecule and not
267 only in the active site. Interestingly, also from the Tn-Seq data, *pbp2* appeared to be considerably
268 less important for growth at 0.5 M NaCl (Supplementary Fig. S5B and S5C), although transposon
269 insertions were mainly located at the beginning and end of the gene or within the promoter region.
270 To confirm that the *pbp2* SNPs were indeed responsible for the suppression of the salt
271 sensitivity of the *957* mutant, we transferred the *pbp2* SNPs from two strains into a fresh LAC*Δ*957*
272 background by co-transduction of a transposon in a nearby gene (Supplementary Fig. S5D,
273 schematic). As expected, these "recreated" suppressor strains showed also increased salt resistance
274 (Fig. 6C, Supplementary Fig. S6A). In addition, we repaired the *pbp2* gene in two suppressors to the
275 WT *pbp2* allele and this reduced their ability to cope with NaCl stress, all consistent with the
276 hypothesis that the SNPs in *pbp2* are responsible for the suppression phenotype (Fig. 6D,
277 Supplementary Fig. S6B). When the same *pbp2* SNPs were transferred into a WT LAC* strain, a
278 reproducible growth improvement of the SNP-bearing strains was observed in high salt medium, an
279 indication that the *pbp2* mutations lead to a general growth improvement of *S. aureus* under NaCl
280 stress conditions (Fig. 6E, Supplementary Fig. S6C). Overall these results show that several
281 independent mutations in the *pbp2* gene can suppress the salt sensitivity of the *957* mutant and can
282 improve growth of the WT strain.

283 **Mutations in the *pbp2* gene alter moenomycin susceptibility and result in reduced peptidoglycan**
284 **crosslinking**

285 Moenomycin is a phosphoglycolipid antibiotic that inhibits the transglycosylase activity of the
286 *S. aureus* Pbp2 enzyme (reviewed in (Ostash & Walker, 2010)). To test if a decrease in Pbp2
287 transglycosylase activity results in improved growth of the *957* mutant in high salt conditions, cells
288 were grown on LB agar containing 0.5 M NaCl with or without moenomycin. The growth behaviors
289 of the WT strain and the *957* mutant were similar when grown on solid LB agar containing 0.5 M
290 NaCl but lacking moenomycin (Fig. 7A, top panel). This discrepancy in the growth behavior of the
291 *957* mutant in high salt liquid versus solid medium was already noted when we attempted to
292 generate suppressors on agar plates. On the other hand, in medium supplemented with 0.02 µg/ml
293 moenomycin, we observed better growth of the *957* mutant compared to the WT strain (Fig. 7A,
294 lower panel). In addition, the *957* mutant also showed improved growth compared to the two
295 suppressor strains S2 and S4 when moenomycin was added (Fig. 7A, lower panel). These findings
296 are consistent with the idea that a partial inhibition of the glycosyltransferase activity of Pbp2 can
297 improve the growth of the *957* mutant in high salt medium.

298 Because the LAC*Δ*957* strain showed increased peptidoglycan crosslinking when compared to
299 a WT strain, we hypothesized that the peptidoglycan of the suppressor strains would be again less
300 crosslinked. To test this, the peptidoglycan from two of the suppressor strains grown in LB 0.4 M
301 NaCl was isolated, the muropeptide profiles determined and compared to that of the original *957*
302 mutant (Fig. 7B, Supplementary Fig. S6D). As before, the muropeptide profiles looked similar but
303 quantification revealed a significant reduction in crosslinked peptidoglycan fragments and a
304 significantly overrepresentation of monomeric and dimeric fragments in the suppressor strains as
305 compared to the original *957* mutant (Fig. 7B). These results indicate that the amount of crosslinking
306 of the peptidoglycan polymer is an important factor in the salt resistance of *S. aureus* and that
307 dysregulation of peptidoglycan crosslinking can lead to destabilizing effects.

308 **Discussion**

309 Using TN-seq, we successfully identified several unidentified salt tolerance genes in the USA300
310 *S. aureus* LAC* strain and further characterized gene *957,* a gene without previously assigned
311 function. Our results indicate that the gene product is involved in cell envelope homeostasis but
312 likely not WTA attachment and we show that its absence leads to increased crosslinking of the
313 peptidoglycan in the presence of NaCl. Suppressors of a *957* mutant acquired mutations in *pbp2* and
314 the increase in peptidoglycan crosslinking was reversed in such stains. This demonstrates that the
315 synthesis of the peptidoglycan layer is a tightly regulated process that plays an essential role during
316 osmotic stress.

317 TN-seq experiments track the growth ability of single mutants in a mixed population and can
318 therefore quickly and accurately determine genes that are required under certain growth condition.
319 It is however always a concern that a single TN-seq experiment might not be reproducible due to
320 stochastic extinction of individual mutants or certain growth dynamics. In this study, we therefore
321 performed two independent NaCl TN-seq experiments using two different libraries and slightly
322 different experimental setups. Although we detected differences between experiments, overall the
323 data proved to be rather consistent suggesting that a single experiment would be sufficient in many
324 cases.

325 Most of the mutants we identified as NaCl essential in the TN-seq screen, proved to be sensitive
326 to 0.5 M NaCl, confirming the effectiveness of the TN-seq screen (Supplementary Fig. S2). In
327 particular, previously uncharacterized genes such as *SAUSA300_0694*, *mgtE,* and the *957* gene could
328 be identified as essential during NaCl stress and their phenotypes could be complemented (Fig. 2).
329 In our study, we opted not to experimentally validate any of the dispensable genes, as the
330 verification of a growth advantage is more difficult to prove than a growth defect, but these genes
331 will provide interesting starting points for future research. In addition, it will be interesting to

332 investigate higher concentrations of NaCl to see if the same or different genes are flagged as
333 essential and dispensable. Somewhat contradictory, our data indicated, that the c-di-AMP
334 phosphodiesterase enzymes GdpP and Pde2 become dispensable when cells are exposed to high
335 salt conditions. This is in contrast to the reports that construction and propagation of a *dacA* mutant
336 (coding for the cognate c-di-AMP cyclase DacA) is only possible at high salt concentrations (or in
337 defined chemical medium) (Zeden *et al.*, 2018). These findings do however point to an involvement
338 of c-di-AMP in salt mediated osmotic stress adaption in *S. aureus*.

339 Gene *957* was selected for further characterization as part of this study, because it had
340 previously not been linked to NaCl stress and had not been investigated before. Initial tests
341 supported our proposed link to the cell envelope. The differences in CFU/OD correlations of the WT
342 and *957* mutant could be explained by the reduced cell size of the *957* mutant, as this would produce
343 more cells per OD unit. The underlying mechanism as to why *957* mutant cells are smaller in size is
344 still unclear but could be related to changes in peptidoglycan homeostasis.

345 As gene *957* is co-transcribed with *lcpB,* we initially assumed the encoded protein is involved in
346 WTA attachment via LcpB. However, we were unable to demonstrate such a link. Instead the *957*
347 mutant exhibited increased muropeptide crosslinking in the presence of 0.4 M NaCl, which could be
348 suppressed by *pbp2* SNPs suggesting an involvement in peptidoglycan synthesis. We can only
349 speculate if the SNPs identified in *pbp2* increase or inhibit the activity of Pbp2. However, judging by
350 the number of independent SNPs, it seems more likely that the mutations lead to a decrease rather
351 than an increase in transglycosylase activity. In addition, the results from the moenomycin
352 sensitivity experiments using a sublethal antibiotic concentration highlights that partial inactivation
353 of the transglycosylase activity of Pbp2 improves the growth of the *957* strain in high salt conditions.
354 This is consistent with the idea that the obtained *pbp2* SNPs lead to a decrease in transglycosylase
355 activity. The absence of frameshift or non-sense mutations can be explained by the importance of
356 the C-terminal transpeptidase domain of *pbp2* (Pinho *et al.*, 2001) and this is also reflected in the

357 transposon insertion distribution in *pbp2*. Intriguingly, the suppressor mutants show reduced
358 growth compared to the *957* mutant on moenomycin plates, presumably due to transglycosylation
359 activity being reduced to levels that are detrimental to the cell. At this point it is unclear how
360 mutations in the transglycosylase domain alter the muropeptide pattern, since the peptide bonds
361 are made by the transpeptidase, not the transglycosylase domain. We hypothesize that a decrease
362 in the efficiency of the glycosylation activity and slowing down the glycan chain synthesis process
363 will reduce the efficiency of the subsequent transpeptidation process, resulting in decreased
364 peptidoglycan crosslinking in the *pbp2* SNP strains. It is also noteworthy that the *pbp2* gene becomes
365 dispensable under NaCl conditions, an additional indicator that Pbp2 activity needs to be avoided
366 under high salt conditions.

367 Interestingly, the *957* mutant exhibited a slightly higher oxacillin MIC than the WT. This is in
368 contrast to what we expected as MICs are determined in 2% (0.342 M) salt medium and this should
369 lead to a growth disadvantage of the mutant. However, when seen in light of the increase in
370 peptidoglycan crosslinking, this could explain the growth advantage of the *957* mutant in the
371 presence of a beta-lactam antibiotic, as this could counter the inhibition of transpeptidases by
372 oxacillin.

373 Although we were unable to determine the exact molecular mechanism, it is clear from our
374 data that gene *957* is involved in cell wall synthesis either directly or indirectly. Based on these data,
375 we hypothesize that the rigidity of the peptidoglycan cell wall could be an important factor to
376 counter osmotic stresses but further experimental work is needed to explore this in depth.

377 In conclusion, we have identified a number of previously uncharacterized factors involved in
378 the osmotic stress response of *S. aureus,* which in particular highlighted the importance of the cell
379 envelope. The generated data, will also provide a great resource for further studies on the
380 staphylococcal NaCl stress response.

381 **Experimental procedures**

382 **Growth of bacteria**

383 *E. coli* and *S. aureus* strains were streaked from frozen stock onto Lysogenic Broth (LB) or Tryptic
384 Soya agar (TSA) plates, respectively. For all *E. coli* and most *S. aureus* experiments, the bacteria were
385 grown in LB medium (LB normal, LBN, 10 g Tryptone, 5 g Yeast extract, 5 g NaCl) pH 7.5 or LB medium
386 with extra 0.5 M NaCl added. For molecular cloning and some other experiments (as indicated in
387 the text), *S. aureus* strains were grown in TSB medium. Growth curves were done in 125 ml flasks
388 with 20 ml of medium without antibiotics. Cultures were inoculated from overnight cultures to a
389 starting OD_{600} of 0.01 and growth was followed by determining OD_{600} readings every one or two
390 hours.

391 **TN-seq experiments**

392 A previously published highly-saturated *S. aureus* USA300 library with a mix of six different
393 transposons was used (Santiago *et al.*, 2015, Coe *et al.*, 2019) for replicate A. For replicate B, a new
394 transposon library with only the blunt transposon was produced using the same techniques as
395 described in Santiago *et al.* (Santiago *et al.*, 2015). This library contained approximately 1.2 million
396 individual clones.

397 For each experiment, one tube of the transposon library was thawed on ice and used to set up
398 a 20 ml pre-culture in LBN/Erm 5 µg/ml with a starting OD_{600} of 0.1. In the case of replicate A, Erm
399 was added throughout all following cultivation steps, whereas Erm was not added to replicate B
400 after the pre-culture. The resulting starter culture was grown for 1 hour and subsequently used to
401 inoculate 25 ml of either LBN or LB 0.5 M to a starting OD_{600} of 0.00125. When the cultures reached
402 an OD_{600} of approximately 0.3, the cultures were back-diluted 1:100-fold into 40 ml fresh medium
403 and 10-12 ml harvested by centrifugation when the back-diluted culture reached an OD_{600} of approx.

404 1.4 (17 generations). The bacterial pellets were washed once with their respective growth medium
405 and stored at -20°C for further processing.

406 The library preparation for sequencing was done as described previously (Santiago *et al.*, 2015).
407 Briefly, genomic DNA was isolated, cut with *Not*I, biotinylated adapters ligated, the DNA cut again
408 with *Mme*I, and fragments ligated to Illumina adapters and the products PCR amplified,
409 incorporating bar codes and the Illumina adaptor sequences P5 and P7. The samples were
410 sequenced on an Illumina HiSeq machine after spiking with 40% PhiX DNA. The data analysis was
411 done using the Tufts Galaxy Server and custom python scripts as described earlier (Santiago *et al.*,
412 2015). To this end, the reads were trimmed up to the barcode and de-multiplexed by strain barcode.
413 Due to the variability in the DNA cleavage by the *Mme*I restriction enzyme, the reads that could not
414 be mapped to a barcode were trimmed by an additional base and the process repeated. Reads were
415 then mapped to the USA300_TCH1516 (CP000730.1) genome and a hop table was generated.
416 Statistical analysis (Mann-Whitney tests and Benjamini-Hochberg) was done using custom python
417 scripts (Santiago *et al.*, 2015). Further exploration of the data was done using Excel and custom R
418 scripts.

419 ***S. aureus* cell diameter measurements**

420 For cell diameter measurements, *S. aureus* strains ANG4054, ANG4340, ANG4341 were grown
421 overnight (14-20 hours) at 37°C with 180 rpm shaking in 5 ml LBN in the presence of 100 ng/ml Atet.
422 100 µl of these overnight cultures was transferred to a 1.5 ml reaction tube and 1.5 µl of BODIPY-
423 FL-vancomycin (100 µg/ml in phosphate buffered saline) was added to each tube to stain the cell
424 wall. After a 30 min static incubation step at 37°C, 1.5 µl of the suspension was pipetted onto a slide
425 covered with a 1% agarose pad and analyzed by microscopy using an Axio Imager.A2 microscope
426 with an EC Plan-Neofluar 100x/1.30 Oil M27 objective and images recorded using an AxioCam MR
427 R3. Native CZI files were opened in FIJI (Schindelin *et al.*, 2012) and cell diameters of 200 cells were

428 measured using the line and measure tool. Only cells without any visible septa were measured.
429 Experiment was conducted five times with independent biological cultures (n=5, 200 cells each).

430 **CFU/OD correlations**

431 The different *S. aureus* strains were grown as described for the cell diameter measurements.
432 Optical densities of cultures were measured as well as 100 µl of 10^{-6} dilutions (made in their
433 respective growth medium) plated onto TSA plates. The next day, the number of colonies were
434 counted and the ratios of OD_{600} to CFU calculated. The experiment was conducted six time with
435 independent biological samples (n=6).

436 **Zymogram assays**

437 The different *S. aureus* strains were grown over night in TSB. The next day, the bacteria from an
438 OD_{600} equivalent of 20 were pelleted by centrifugation for 3 min at 17000 x *g*. The cells were washed
439 twice with 600 µl PBS and subsequently suspended in 50 µl SDS sample buffer. The suspension was
440 boiled for 20 min with interspersed shaking, centrifuged for 5 min at 17000 x *g* and 20 µl of each
441 sample was loaded onto Zymogram gels, which where were prepared as described previously
442 (Atilano *et al.*, 2014). Gels were stained and de-stained using methylene blue and water. The
443 experiment was performed twice, and a representative result is shown.

444 **WTA isolation and analysis**

445 Overnight cultures of *S. aureus* strains ANG4054, ANG4340, ANG4341, ANG1575, ANG4290,
446 ANG4748, ANG4749, ANG4759 were prepared in LBN and used to inoculate 50 ml LBN or LB 0.4 M
447 NaCl to an OD_{600} of 0.01. The cultures were incubated at 37°C with shaking until they reached an
448 OD_{600} of 5 to 6. Where appropriate, 10 µg/ml chloramphenicol and 100 ng/ml Atet was also added

449 to the medium. The bacteria from 20-24 ml culture were harvested by centrifugation for 10 min at
450 7000 x *g*. The bacterial pellets were washed with 50 mM 2-(N-morpholino) ethanesulfonic acid
451 (MES) pH 6.5 buffer and stored at -20°C until further use. Pellets were then processed and WTA
452 separated on a 20% native polyacrylamide gel by electrophoresis on a Biorad Protein XL ii cell as
453 described previously (Covas *et al.*, 2016) and WTA visualized by silver staining according to the
454 manufacturer protocol. Experiments were done with three biological replicates (n=3) and a
455 representative result is shown.

456 **Peptidoglycan isolation and analysis**

457 Peptidoglycan was prepared as described previously (Corrigan *et al.*, 2011) with the following
458 modifications: 0.5 L (ANG4290, ANG4382, ANG4384) or 1.0 L (ANG5054, ANG4340, ANG4341) of LB
459 0.4 M NaCl medium (all strains) or LBN (ANG5054, ANG4340, ANG4341) medium were inoculated
460 to an OD_{600} of 0.01. For strains carrying derivatives of plasmid piTET, the medium was supplemented
461 with 100 ng/ml Atet starting from the pre-cultures. The cultures were grown at 37°C with shaking
462 at 180 rpm until they reached an OD_{600} of 2-3 and bacteria were subsequently harvested by
463 centrifugation. Chromatography of mutanolysin digested peptidoglycan was performed as
464 described previously using an Agilent 1260 infinity system (Corrigan *et al.*, 2011) and muropeptide
465 peaks assigned according to de Jonge *et al.* (de Jonge *et al.*, 1992). For the muropeptide
466 quantification, a baseline was drawn, the total peak area determined as well as the peak areas for
467 mono- and the different multimer peaks and calculated as percentage of the total peak area. The
468 peak area quantification was done three times for each HPLC chromatogram and average values
469 were calculated. Experiments were done with three biological replicates (n=3).

470 **Data analysis, software and statistics**

471 Data were processed with a combination of Python 3.6 (https://www.python.org), R 3.3 & 3.5
472 (https://www.r-project.org/), RStudio 1.1 & 1.2 (https://www.rstudio.com/), Prism 7 and 8
473 (https://www.graphpad.com), ChemStation OpenLab C.01.05 (https://www.agilent.com/) and
474 Microsoft Excel 15 and 16 (https://www.office.com/). Microscopy images were analyzed using FIJI
475 1.0 (https://fiji.sc/). Statistical analysis was performed with Prism using appropriate tests as
476 described in the figure legends.

477 **Raising of Δ*957* suppressor strains**

478 Multiple independent overnight cultures of strain LAC*Δ*957* (ANG4290) were prepared in 5 ml
479 LBN. These cultures were back diluted the next day into 20 ml LB 0.5 M NaCl to a starting OD_{600} of
480 0.05 and grown for 8-10 hours at 37°C with shaking until the cultures were slightly turbid. 50 µl of
481 each culture was passed into 5 ml of LBN and grown overnight. The next day, appropriate culture
482 dilutions were plated onto LBN agar plates and incubated overnight at 37°C. For each independent
483 culture, multiple single colonies were picked and used to inoculate individual wells of a 96-well
484 microtiter plates containing 100 µl LBN and the plates were subsequently incubated at 37°C in a 96-
485 well plate incubator with shaking at 650 rpm. The next day, a culture aliquot was stored at -80°C,
486 and the cultures were also diluted 1:50 in LB 0.5 M NaCl medium and 20 µl of these diluted cultures
487 used to inoculate 180 µl of LB 0.5 M NaCl medium. The plates were incubated overnight with shaking
488 at 37°C and the next morning the growth of the potential *957* suppressor strains compared to that
489 of the original LAC*Δ*957* deletion strain (ANG4290), which showed low growth and the WT LAC*
490 (ANG1575) strain, which showed good growth. For each lineage, four suppressors that showed good
491 growth were streaked out from the previously frozen stocks and subsequently single colonies
492 selected to set up overnight cultures. The deletion of gene *SAUSA300_0957* was confirmed by PCR

493 and after performing growth curves in culture flasks, one strain that showed significant growth
494 improvement compared to the original LAC*Δ*957* (ANG4290) strain was selected from each lineage.
495 These strains were streaked out again for single colonies and used to inoculate an overnight culture,
496 giving rise to the independently raised suppressor strains ANG4381 through ANG4394. The
497 compensatory mutations for several of these suppressor strains were subsequently determined by
498 whole genome sequencing.

499 **Transfer of *pbp2* SNPs by phage transduction**

500 In order to demonstrate that the SNPs in *pbp2* are responsible for the growth rescue of strain
501 LAC*Δ*957* (ANG4290), we transferred two different *pbp2* SNPs by phage transduction into the
502 original LAC*Δ*957* strain as well as repaired these SNPs in the suppressor strains. This was done by
503 placing an Erm-marked transposon in proximity of the *pbp*2 gene allowing at a certain frequency for
504 the co-transduction of the Erm marker and the *pbp2* SNP. To this end, the NTML transposon mutant
505 library strain NE789 (Fey *et al.*, 2013) was used, which harbors a transposon insertion in
506 *SAUSA300_1332* (putative exonuclease) about 10 kbp upstream of the *pbp2* gene. *SAUSA300_1332*
507 is expected to be unrelated to salt stress and the cell wall synthesis machinery but close enough to
508 lead to an intermediate rate of co-transference with the *pbp2* SNPs. The transposon from NE789
509 was transduced into WT LAC* (Boles *et al.*, 2010) and strain LAC*Δ*957* (ANG4290) using phage Φ85
510 yielding strains ANG4561 and ANG452, respectively. The transposon was also transduced into the
511 suppressor strains ANG4382 and ANG4384 transferring either *SAUSA300_1332::Tn* only, yielding
512 strains ANG4527 and 4528 or transferring *SAUSA300_1332::Tn* as well as replacing the *pbp2* SNP
513 with a WT *pbp2* allele yielding *pbp2* repaired strains ANG4557 and ANG4568. Lysates from strains
514 ANG4527 and 4528 (suppressors containing *pbp2* SNPs and *SAUSA300_1332::Tn*) were used to
515 transfer the *pbp2* SNPs back into a clean LAC*Δ*957* strain background yielding strains ANG4624 and
516 ANG4625 and into WT LAC*, yielding strains ANG4563 and ANG4564. Successful repair or transfer

517 of the SNPs was checked by PCR and subsequent restriction digest of the product choosing enzymes
518 that recognize sites present in either the WT or SNP allele (ANG4382 *pbp2* SNP: BsrI. Recognition
519 site CCWGG, additional site introduced by SNP; ANG4384 *pbp2* SNP: SspI. Recognition site: AATATT,
520 site missing in SNP).

521 **Determination of oxacillin MICs using Etest strips**

522 *S. aureus* strains LAC* piTET (ANG4054), LAC*Δ*957* piTET (ANG4340) and the complementation
523 strain LAC*Δ*957* piTET-*957* (ANG4341) were grown overnight (22 hours) in 5 ml TSB containing 10
524 µg/ml chloramphenicol and 100 ng/ml Atet. The next day, the cultures were diluted to an OD_{600} of
525 0.1 in sterile PBS buffer and streaked with cotton swabs onto cation adjusted Mueller-Hinton agar
526 plates supplemented with 2% NaCl and 100 ng/ml Atet. One M.I.C.Evaluator strip was placed on
527 each plate and the plates were incubated for 24 hours at 35°C. MICs were then read directly from
528 the strips. The experiment was done with 4 biological replicates (n=4).

529 **Moenomycin growth improvement test**

530 *S. aureus* strains LAC* (ANG1575), LAC* Δ*957* (ANG4290), LAC* Δ*957* S2 (ANG4382) and LAC*
531 Δ*957* S4 (ANG4384) were grown overnight (18 hours) in 5 ml LBN. The next day, the cells were
532 diluted to an OD_{600} of 0.01 in LBN, grown until mid-exponential phase (OD_{600} 0.4-0.6) and normalized
533 to an OD_{600} of 0.1. The cells were 10-fold serially diluted and 5 µl of each dilution spotted onto LB
534 agar containing 0.5 M NaCl with either 0.02 µg/ml moenomycin (mix of moenomycin A, A12, C1, C3
535 and C4, Santa Cruz Biotechnology) or no moenomycin. Plates were incubated at 37°C overnight (18-
536 22 hours) and photographed. The experiment was done with 3 biological replicates (n=3) and one
537 representative result is shown.

538 **Whole genome sequencing**

539 Genomic DNA was either isolated using the Promega Gene Wizard kit according to the
540 manufacturer instructions or using chloroform-isoamylalcohol as described previously (Schuster &
541 Bertram, 2014). DNA was sent off for whole genome sequencing to MicrobesNG, Birmingham, U.K.
542 or libraries prepared using the Illumina Nextera DNA kit and sequenced at the London Institute of
543 Medical Sciences. Short reads were trimmed in CLC workbench genomics (Qiagen), then mapped to
544 a custom *S. aureus* USA300 LAC* reference genome generated in a previous study (Bowman *et al.*,
545 2016) and single nucleotide polymorphisms called based on at least 80% frequency of occurrence.
546 This list was compared to a manually curated list of well non false-positives and these entries were
547 removed.

548 **Nebraska Transposon Mutant Library (NTML) strains and complementation strains**

549 All Nebraska transposon mutant library (NTML) strains and primers used in this study are listed
550 in Supplementary Tables S9, S11 and S12. Transposon insertions in the respective genes were
551 confirmed by PCRs. For complementation analysis, NTML strains NE535 (JE2 *SAUSA300_0867*::*Tn*),
552 NE867 (JE2 *SAUSA300_0483*::*Tn*) were transformed as controls with the empty plasmid pCL55 (Lee
553 *et al.*, 1991), yielding strains ANG4326 and ANG4328 and strains NE188 (JE2 *SAUSA300_0481*::*Tn*),
554 NE251 (JE2 SAUSA300_0482::*Tn*), NE526 (JE2 *SAUSA300_0694*::*Tn*), NE736 (JE2
555 *SAUSA300_0910*::*Tn*), NE1384 (JE2 *SAUSA300_0957*::*Tn*) with plasmid piTET (Gründling &
556 Schneewind, 2007), yielding ANG4308, ANG4310, ANG4377, ANG4336, ANG4338. The WT strain JE2
557 (Fey *et al.*, 2013) was also transformed with both plasmids yielding JE2 pCL55 (ANG4325) and JE2
558 piTET (ANG4307).

559 The complementation plasmid piTET-*481* for strain NE188 (JE2 *SAUSA300_0481::Tn*) was
560 constructed by amplifying the *SAUSA300_0481* gene using primers P2378/P2379, digesting the

561 product with AvrII/BglII and ligating the fragment with plasmid piTET cut with the same enzymes.
562 The plasmid was then introduced into *E. coli* strain XL1-Blue, yielding ANG4139. After shuttling the
563 plasmid through *E. coli* strain IM08B (Monk *et al.*, 2012), creating strain ANG4150, the plasmid was
564 integrated into the *geh* locus of NE188 (JE2 *SAUSA300_0481*::*Tn*) yielding strain ANG4309. The
565 complementation plasmid piTET-*482* for strain NE251 (JE2 SAUSA300_0482::*Tn*), piTET-*694* for
566 strain NE526 (JE2 *SAUSA300_0694*::*Tn*), piTET-*910* for strain NE736 (JE2 *SAUSA300_0910*::*Tn*), and
567 piTET-*957* for strain NE1384 (JE2 *SAUSA300_0957*::*Tn*) were constructed in a similar manner using
568 primer pairs P2380/P2381 (*SAUSA300_0482*), P2388/P2389 (*SAUSA300_0694*), P2384/P2385
569 (*SAUSA300_0910*) and P2386/P2387 (*SAUSA300_0957*), respectively. The complementation
570 plasmids were recovered in *E. coli* XL1-Blue yielding strains ANG4140 (SAUSA300_0482), ANG4142
571 (*SAUSA300_0694*), ANG4144 (*SAUSA300_0910*) and ANG4145 (*SAUSA300_0957*), shuttled through
572 *E. coli* IM08B giving strains ANG4151 (*SAUSA300_0482*), ANG4153 (*SAUSA300_0694*), ANG4155
573 (*SAUSA300_0910*) and ANG4156 (*SAUSA300_0957*) and finally introduced in the respective NTML
574 strain yielding the complementation strains ANG4311 (*SAUSA300_0482*), ANG4378
575 (*SAUSA300_0694*), ANG4337 (*SAUSA300_0910*) and ANG4339 (*SAUSA300_0957*).
576 Complementation plasmid pCL55-*483* for strain NE867 (JE2 *SAUSA300_0483*::*Tn*) was made by
577 fusing PCR products of the operon promoter (in front of *SAUSA300_0481*) amplified with primers
578 P2588/P2553 and the *SAUSA300_0483* gene, amplified with primers P2554/P2589 together using
579 primers P2588/P2589. The resulting fragment was cloned into pCL55 using EcoRI/BamHI restriction
580 sites. The plasmid was recovered in XL1-Blue, creating strain ANG4291, shuttled through *E. coli*
581 IM08B (ANG4292) and subsequently introduced into NE867 (JE2 *SAUSA300_0483*::*Tn*) to create
582 strain ANG4327. The complementation plasmid pCL55-*867* for strain NE535 (JE2
583 *SAUSA300_0867*::*Tn*) was constructed in a similar manner, using primers P2590/P2556 and
584 P2557/P2591 to amplify the promoter and *SAUSA300_0867* gene, which were subsequently fused
585 in a second PCR using primers P2590/P2591. The resulting fragment was cloning into pCL55 using

586 EcoRI/BamHI restriction sites and the resulting plasmid recovered in *E. coli* XL1-Blue (ANG4293),
587 shuttling through IM08B (ANG4294) and finally introduced into NE535 (JE2 *SAUSA300_0867*::*Tn*),
588 creating the complementation strain ANG4329.

589 **Construction of *S. aureus* gene deletion and complementation strains**

590 *S. aureus* strains with in-frame gene deletions were constructed by allelic exchange using
591 plasmids pIMAY (Monk *et al.*, 2012) and pIMAY* (Schuster *et al.*, 2019). The gene deletion plasmids
592 were designed to contain approximately 1000 bp up- and downstream regions around the deletion
593 site, amplified from LAC* genomic DNA (Boles *et al.*, 2010), and the first and last 30 bp of the open
594 reading frame to be deleted.

595 For construction of plasmid pIMAY-Δ*957*, the up- and downstream regions of *SAUSA300_0957*
596 were amplified using primers P2370/P2371 and P2372/P2373, spliced together in a second PCR
597 using primers P2370/P2373 and cloned into pIMAY using XmaI/EcoRI. Plasmid pIMAY-Δ957 was
598 recovered in *E. coli* XL1-Blue, creating strain ANG4147, shuttled through *E. coli* IM08B (ANG4159)
599 and subsequently introduced into S*. aureus* LAC*Δ*957*. The allelic exchange to delete
600 *SAUSA300_0957* and to create strain LAC*Δ*957* (ANG4290) was performed as previously described
601 (Monk *et al.*, 2012). For complementation analysis, plasmid piTET-*957* was integrated into the
602 chromosome of strain LAC*Δ*957*, giving rise to the complementation strain LAC*Δ*957* piTET-*957*
603 (ANG4341). As control, the empty plasmid piTET from ANG4163 was also integrated into the
604 chromosome of LAC*Δ*957* yielding strain LAC*Δ*957* piTET (ANG4340). The *lcpB* (SAUSA300_0958)
605 gene was deleted in a similar manner using primers P2844/P2845 and P2846/P2847 for the first and
606 primers P2844/P2847 for the second PCR and cloning the fragment XmaI/EcoRI into pIMAY. Plasmid
607 pIMAY-Δ*lcpB* was recovered in *E. coli* XL1blue (ANG4740), shuttled through *E. coli* IM08B (ANG4742)
608 and introduced into the *S. aureus* LAC* (ANG4744) and finally yielding the *lcpB* deletion strain
609 LAC*Δ*lcpB* (ANG4748).

610 Plasmid pIMAY*-Δ*957-958* was constructed for the production of an *SAUSA300_0957-0958*
611 (*lcpB*) double mutant strain in which the first 30 bases of *SAUSA300_0957* were fused to the last 30
612 bp of *SAUSA300_0958* (*lcpB*). This was done using primers P2844/P2848 and P2849/P2373 in the
613 first and primers P2844/P2373 in a second PCR. The fragment was cloned using XmaI/EcoRI into
614 pIMAY* (Schuster *et al.*, 2019) and the resulting plasmid pIMAY*-Δ*957-958* recovered in *E. coli* XL1-
615 Blue (ANG4741). The plasmid was shuttled through *E. coli* IM08B (ANG4743), introduced into *S.*
616 *aureus* LAC* (ANG4745) and following the allelic exchange procedure yielding the *S. aureus* strain
617 LAC*Δ*957-958* (*lcpB*) (ANG4749).

618 The plasmid pIMAY-Δ*mgtE* was designed to contain up- and downstream regions of
619 *SAUSA300_0910* (*mgtE*) fused together by the first and last 30 bp of the gene in order to create a
620 LAC*Δ*mgtE* mutant. For this, primer pairs P2374/P2375 and P2376/P2377 were used to amplify up-
621 and downstream regions and subsequently spliced together by PCR using primers P2374/P2377.
622 The PCR fragment was digested with XmaI/EcoRI and ligated into pIMAY cut with the same enzymes.
623 The plasmid pIMAY-Δ*mgtE* was recovered in *E. coli* XL1-Blue yielding strain ANG4146 and shuttled
624 through *E. coli* IM08B yielding strain ANG4158. The plasmid pIMAY-Δ*mgtE* was then introduced into
625 LAC* yielding strain LAC*Δ*SAUSA300_0910* (*mgtE*) (ANG4422) after the knockout procedure. To
626 create an empty vector-containing control strain and a plasmid-based complementation strain, the
627 plasmid piTET and piTET-*910* from strains ANG4163 and ANG4155 were isolated and used to
628 transform strain LAC*Δ*SAUSA300_0910* (*mgtE*) (ANG4422), yielding strains ANG4445 (LAC*Δ*mgtE*
629 piTET) and ANG4446 (LAC*Δ*mgtE* piTET-*mgtE)*.

630 The *tagO* gene (*SAUSA300_0731*) was inactivated using the targetron intron homing system
631 (Yao *et al.*, 2006) or by allelic exchange using pIMAY* (Schuster *et al.*, 2019). For the targetron
632 mutagenesis, plasmid pNL9164-*tagO* was produced by amplifying the upstream targetron fragment
633 with primers P2887 and the EBS universal primer (P2890) and the downstream fragment using
634 primers P2888/P2889, the fragments were fused using the IBS primer (P2887) and the EBS1d primer

635 (P2888). The final fragment was cloned using HindIII/BsrGI into pNL9164 (Yao *et al.*, 2006). Plasmid
636 pNL9164-*tagO* was recovered in *E. coli* XL1-Blue, yielding strain ANG4703, introduced into *E. coli*
637 IM08B to give rise to strain ANG4704 and finally introduced into *S. aureus* LAC* (Boles *et al.*, 2010)
638 to create strain LAC* pNL9164-*tagO* (ANG4751). The final *tagO* targetron mutant strain
639 LAC**tagO*::targetron (ANG4753) was generated using the method described by Yao *et al.* (Yao *et*
640 *al.*, 2006). For the construction of *S. aureus* strain LAC*Δ*tagO* with an in-frame deletion in *tagO,* the
641 allelic exchange plasmid pIMAY*-Δ*tagO* was used. To this end, up- and downstream *tagO* fragments
642 were produced using primer pairs P2883/P2884 and P2885/P2886 and introduced by Gibson cloning
643 into XmaI/EcoRI pre-cut pIMAY*. Plasmid pIMAY*-Δ*tagO* was recovered in *E. coli* XL1-Blue,
644 generating strain ANG4755. After shuttling through *E. coli* strain IM08B (ANG4756), the plasmid was
645 introduced into *S. aureus* LAC* to create strain ANG4757. Finally, the *tagO* locus was deleted by
646 allelic exchange, generating strain LAC*Δ*tagO* (ANG4759). Because initial generation of the mutant
647 failed, cells were plated unselectively onto TSA plates and incubated at room temperature (18-25°C)
648 for about two weeks to enable colony differentiation between WT and Δ*tagO* mutant strains. Upon
649 prolonged incubation, *tagO* mutant strain colonies have an opaque appearance.

650 **Data access**

651 The whole genome sequencing data were deposited at the European Nucleotide Archive (ENA)
652 under accession id ERP115099 and TN-seq data in the short read archive (SRA) at the National
653 Center for Biotechnology Information (NCBI) under BioProject ID PRJNA544248. Analyzed tables can
654 be found in the supplementary files. For other data, please contact the corresponding author.

655 **Acknowledgements**

656 This research was funded by the Wellcome Trust through grants 100289 and 210671/Z/18/Z to
657 A.G. and the NIH grant P01AI083214 to S.W.. C.F.S. was supported by the German Research

658 Foundation [Deutsche Forschungsgemeinschaft (DFG)] through grant SCHU 3159/1–1 and F.C.M.K.
659 by a Wellcome trust Ph.D. studentship. The funders had no role in study design, data collection and
660 analysis, decision to publish, or preparation of the manuscript. We thank Microbes NG and the
661 London Institute of Medical Sciences for providing whole genome sequencing services and the Tufts
662 sequencing facility for the sequencing services for the TN-seq experiments. We also would like to
663 thank Ute Bertsche for kind advice on HPLC analyses.

664 **Author contributions**

665 C.F.S., D.M.W., F.C.K. and A.G. performed the research; C.F.S., D.M.W., F.C.M.K., M.S., S.W. and
666 A.G. analyzed the data; C.F.S. and A.G. designed the research; C.F.S. and A.G. wrote the paper. All
667 authors approved the final version of the manuscript.

668

669 **Disclosure declaration**

670 The authors declare not conflict of interest.

671 **Graphical abstract**

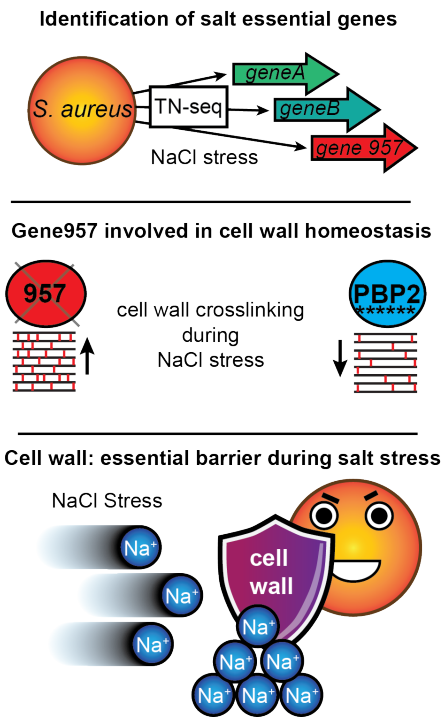

672

673 **Abbreviated summary**

674 *Staphylococcus aureus* is able to grow in the presence of high concentrations of NaCl but the
675 exact genetic factors contributing to this are unknown. Using a high-throughput TN-seq approach,
676 we identified gene *957* as an important factor for the salt stress resistance in *S. aureus*. A *957*-
677 mutant was not only salt sensitive but also showed increased peptidoglycan crosslinking, altogether
678 highlighting the cell wall as an important barrier against osmotic stress.

679

680

681 **References**

682 Adams, M.R., and Moss, M.O., (2008) 7.14.2 The Organism and its Characteristics. In: Food
683 Microbiology (3rd Edition). Royal Society of Chemistry, pp.
684 Anderson, C.B., and Witter, L.D. (1982) Glutamine and proline accumulation by *Staphylococcus*
685 *aureus* with reduction in water activity. *Appl Environ Microbiol* **43**: 1501-1503.
686 Atilano, M.L., Pereira, P.M., Vaz, F., Catalão, M.J., Reed, P., Grilo, I.R., Sobral, R.G., Ligoxygakis, P.,
687 Pinho, M.G., and Filipe, S.R. (2014) Bacterial autolysins trim cell surface peptidoglycan to
688 prevent detection by the *Drosophila* innate immune system. *Elife* **3**: e02277.
689 Bae, J.H., and Miller, K.J. (1992) Identification of two proline transport systems in *Staphylococcus*
690 *aureus* and their possible roles in osmoregulation. *Appl Environ Microbiol* **58**: 471-475.
691 Berger-Bächi, B., Barberis-Maino, L., Strässle, A., and Kayser, F.H. (1989) FemA, a host-mediated
692 factor essential for methicillin resistance in *Staphylococcus aureus*: molecular cloning and
693 characterization. *Mol Gen Genet* **219**: 263-269.
694 Boles, B.R., Thoendel, M., Roth, A.J., and Horswill, A.R. (2010) Identification of genes involved in
695 polysaccharide-independent *Staphylococcus aureus* biofilm formation. *PLoS One* **5**: e10146.
696 Booth, I.R. (2014) Bacterial mechanosensitive channels: progress towards an understanding of their
697 roles in cell physiology. *Curr Opin Microbiol* **18**: 16-22.
698 Bowman, L., Zeden, M.S., Schuster, C.F., Kaever, V., and Gründling, A. (2016) New Insights into the
699 Cyclic Di-adenosine Monophosphate (c-di-AMP) Degradation Pathway and the Requirement
700 of the Cyclic Dinucleotide for Acid Stress Resistance in *Staphylococcus aureus*. *J Biol Chem*
701 **291**: 26970-26986.
702 Bremer, E., and Krämer, R. (2019) Responses of Microorganisms to Osmotic Stress. *Annu Rev*
703 *Microbiol* **73**: 313-334.
704 Brown, S., Santa Maria, J.P., Jr., and Walker, S. (2013) Wall teichoic acids of gram-positive bacteria.
705 *Annu Rev Microbiol* **67**: 313-336.
706 Chan, Y.G., Frankel, M.B., Dengler, V., Schneewind, O., and Missiakas, D. (2013) *Staphylococcus*
707 *aureus* mutants lacking the LytR-CpsA-Psr family of enzymes release cell wall teichoic acids
708 into the extracellular medium. *J Bacteriol* **195**: 4650-4659.
709 Chan, Y.G., Kim, H.K., Schneewind, O., and Missiakas, D. (2014) The capsular polysaccharide of
710 *Staphylococcus aureus* is attached to peptidoglycan by the LytR-CpsA-Psr (LCP) family of
711 enzymes. *J Biol Chem* **289**: 15680-15690.
712 Christian, J.H., and Waltho, J.A. (1964) The Composition of *Staphylococcus aureus* in Relation to the
713 Water Activity of the Growth Medium. *J Gen Microbiol* **35**: 205-213.
714 Coe, K.A., Lee, W., Komazin-Meredith, G., Meredith, T.C., Grad, Y.H., and Walker, S. (2019)
715 Comparative Tn-Seq reveals common daptomycin resistance determinants in
716 *Staphylococcus aureus* despite strain-dependent differences in essentiality of shared cell
717 envelope genes. *bioRxiv*: 648246.
718 Commichau, F.M., Gibhardt, J., Halbedel, S., Gundlach, J., and Stülke, J. (2018) A Delicate
719 Connection: c-di-AMP Affects Cell Integrity by Controlling Osmolyte Transport. *Trends*
720 *Microbiol* **26**: 175-185.
721 Corrigan, R.M., Abbott, J.C., Burhenne, H., Kaever, V., and Gründling, A. (2011) c-di-AMP is a new
722 second messenger in *Staphylococcus aureus* with a role in controlling cell size and envelope
723 stress. *PLoS Pathog* **7**: e1002217.
724 Corrigan, R.M., Campeotto, I., Jeganathan, T., Roelofs, K.G., Lee, V.T., and Gründling, A. (2013)
725 Systematic identification of conserved bacterial c-di-AMP receptor proteins. *Proc Natl Acad*
726 *Sci U S A* **110**: 9084-9089.
727 Corrigan, R.M., and Gründling, A. (2013) Cyclic di-AMP: another second messenger enters the fray.
728 *Nat Rev Microbiol* **11**: 513-524.

729 Covas, G., Vaz, F., Henriques, G., Pinho, M.G., and Filipe, S.R. (2016) Analysis of Cell Wall Teichoic
730 Acids in *Staphylococcus aureus*. *Methods Mol Biol* **1440**: 201-213.
731 Cox, C.D., Bavi, N., and Martinac, B. (2018) Bacterial Mechanosensors. *Annu Rev Physiol* **80**: 71-93.
732 Csonka, L.N. (1989) Physiological and genetic responses of bacteria to osmotic stress. *Microbiol Rev*
733 **53**: 121-147.
734 Csonka, L.N., and Hanson, A.D. (1991) Prokaryotic osmoregulation: genetics and physiology. *Annu*
735 *Rev Microbiol* **45**: 569-606.
736 de Jonge, B.L., Chang, Y.S., Gage, D., and Tomasz, A. (1992) Peptidoglycan composition of a highly
737 methicillin-resistant *Staphylococcus aureus* strain. The role of penicillin binding protein 2A. *J*
738 *Biol Chem* **267**: 11248-11254.
739 Fey, P.D., Endres, J.L., Yajjala, V.K., Widhelm, T.J., Boissy, R.J., Bose, J.L., and Bayles, K.W. (2013) A
740 genetic resource for rapid and comprehensive phenotype screening of nonessential
741 *Staphylococcus aureus* genes. *MBio* **4**: e00537-00512.
742 Graham, J.E., and Wilkinson, B.J. (1992) *Staphylococcus aureus* osmoregulation: roles for choline,
743 glycine betaine, proline, and taurine. *J Bacteriol* **174**: 2711-2716.
744 Gründling, A., and Schneewind, O. (2007) Genes required for glycolipid synthesis and lipoteichoic
745 acid anchoring in *Staphylococcus aureus*. *J Bacteriol* **189**: 2521-2530.
746 Gunde-Cimerman, N., Plemenitas, A., and Oren, A. (2018) Strategies of adaptation of
747 microorganisms of the three domains of life to high salt concentrations. *FEMS Microbiol Rev*
748 **42**: 353-375.
749 Holland, L.M., Conlon, B., and O'Gara, J.P. (2011) Mutation of *tagO* reveals an essential role for wall
750 teichoic acids in *Staphylococcus epidermidis* biofilm development. *Microbiology* **157**: 408-
751 418.
752 Ishibashi, M., Kurokawa, K., Nishida, S., Ueno, K., Matsuo, M., and Sekimizu, K. (2007) Isolation of
753 temperature-sensitive mutations in *murC* of *Staphylococcus aureus*. *FEMS Microbiology*
754 *Letters* **274**: 204-209.
755 Jordan, S., Hutchings, M.I., and Mascher, T. (2008) Cell envelope stress response in Gram-positive
756 bacteria. *FEMS Microbiol Rev* **32**: 107-146.
757 Kho, K., and Meredith, T.C. (2018) Salt-Induced Stress Stimulates a Lipoteichoic Acid-Specific Three-
758 Component Glycosylation System in *Staphylococcus aureus*. *J Bacteriol* **200**.
759 Koprivnjak, T., Mlakar, V., Swanson, L., Fournier, B., Peschel, A., and Weiss, J.P. (2006) Cation-
760 induced transcriptional regulation of the dlt operon of *Staphylococcus aureus*. *J Bacteriol*
761 **188**: 3622-3630.
762 Lee, C.Y., Buranen, S.L., and Ye, Z.H. (1991) Construction of single-copy integration vectors for
763 *Staphylococcus aureus*. *Gene* **103**: 101-105.
764 Lovering, A.L., De Castro, L., and Strynadka, N.C. (2008) Identification of dynamic structural motifs
765 involved in peptidoglycan glycosyltransfer. *J Mol Biol* **383**: 167-177.
766 Mäder, U., Nicolas, P., Depke, M., Pané-Farré, J., Debarbouille, M., van der Kooi-Pol, M.M., Guérin,
767 C., Dérozier, S., Hiron, A., Jarmer, H., Leduc, A., Michalik, S., Reilman, E., Schaffer, M.,
768 Schmidt, F., Bessières, P., Noirot, P., Hecker, M., Msadek, T., Völker, U., and van Dijl, J.M.
769 (2016) *Staphylococcus aureus* Transcriptome Architecture: From Laboratory to Infection-
770 Mimicking Conditions. *PLoS Genet* **12**: e1005962.
771 Madiraju, M.V., Brunner, D.P., and Wilkinson, B.J. (1987) Effects of temperature, NaCl, and
772 methicillin on penicillin-binding proteins, growth, peptidoglycan synthesis, and autolysis in
773 methicillin-resistant *Staphylococcus aureus*. *Antimicrob Agents Chemother* **31**: 1727-1733.
774 Measures, J.C. (1975) Role of amino acids in osmoregulation of non-halophilic bacteria. *Nature* **257**:
775 398-400.
776 Miller, K.J., Zelt, S.C., and Bae, J.-H. (1991) Glycine betaine and proline are the principal compatible
777 solutes of *Staphylococcus aureus*. *Current Microbiology* **23**: 131-137.

778 Mistretta, N., Brossaud, M., Telles, F., Sanchez, V., Talaga, P., and Rokbi, B. (2019) Glycosylation of
779 *Staphylococcus aureus* cell wall teichoic acid is influenced by environmental conditions. *Sci*
780 *Rep* **9**: 3212.
781 Mlynek, K.D., Callahan, M.T., Shimkevitch, A.V., Farmer, J.T., Endres, J.L., Marchand, M., Bayles,
782 K.W., Horswill, A.R., and Kaplan, J.B. (2016) Effects of Low-Dose Amoxicillin on
783 *Staphylococcus aureus* USA300 Biofilms. *Antimicrob Agents Chemother* **60**: 2639-2651.
784 Monk, I.R., Shah, I.M., Xu, M., Tan, M.W., and Foster, T.J. (2012) Transforming the untransformable:
785 application of direct transformation to manipulate genetically *Staphylococcus aureus* and
786 *Staphylococcus epidermidis*. *MBio* **3**.
787 Murakami, K., Fujimura, T., and Doi, M. (1994) Nucleotide sequence of the structural gene for the
788 penicillin-binding protein 2 of *Staphylococcus aureus* and the presence of a homologous
789 gene in other staphylococci. *FEMS Microbiol Lett* **117**: 131-136.
790 Ochiai, T. (2000) *Staphylococcus aureus* produces autolysin-susceptible cell walls during growth in a
791 high-NaCl and low-Ca2+ concentration medium. *Microbiol Immunol* **44**: 97-104.
792 Onyango, L.A., Hugh Dunstan, R., Roberts, T.K., Macdonald, M.M., and Gottfries, J. (2013)
793 Phenotypic variants of staphylococci and their underlying population distributions following
794 exposure to stress. *PLoS One* **8**: e77614.
795 Oshida, T., Sugai, M., Komatsuzawa, H., Hong, Y.M., Suginaka, H., and Tomasz, A. (1995) A
796 *Staphylococcus aureus* autolysin that has an N-acetylmuramoyl-L-alanine amidase domain
797 and an endo-beta-N-acetylglucosaminidase domain: cloning, sequence analysis, and
798 characterization. *Proc Natl Acad Sci U S A* **92**: 285-289.
799 Ostash, B., and Walker, S. (2010) Moenomycin family antibiotics: chemical synthesis, biosynthesis,
800 and biological activity. *Nat Prod Rep* **27**: 1594-1617.
801 Over, B., Heusser, R., McCallum, N., Schulthess, B., Kupferschmied, P., Gaiani, J.M., Sifri, C.D., Berger-
802 Bächi, B., and Stutzmann Meier, P. (2011) LytR-CpsA-Psr proteins in *Staphylococcus aureus*
803 display partial functional redundancy and the deletion of all three severely impairs septum
804 placement and cell separation. *FEMS Microbiol Lett* **320**: 142-151.
805 Pinho, M.G., Filipe, S.R., de Lencastre, H., and Tomasz, A. (2001) Complementation of the essential
806 peptidoglycan transpeptidase function of penicillin-binding protein 2 (PBP2) by the drug
807 resistance protein PBP2A in *Staphylococcus aureus*. *J Bacteriol* **183**: 6525-6531.
808 Pöhlmann-Dietze, P., Ulrich, M., Kiser, K.B., Döring, G., Lee, J.C., Fournier, J.M., Botzenhart, K., and
809 Wolz, C. (2000) Adherence of *Staphylococcus aureus* to endothelial cells: influence of
810 capsular polysaccharide, global regulator agr, and bacterial growth phase. *Infect Immun* **68**:
811 4865-4871.
812 Pourkomailian, B., and Booth, I.R. (1992) Glycine betaine transport by *Staphylococcus aureus*:
813 evidence for feedback regulation of the activity of the two transport systems. *Microbiology*
814 **140 (Pt 11)**: 3131-3138.
815 Price-Whelan, A., Poon, C.K., Benson, M.A., Eidem, T.T., Roux, C.M., Boyd, J.M., Dunman, P.M.,
816 Torres, V.J., and Krulwich, T.A. (2013) Transcriptional profiling of *Staphylococcus aureus*
817 during growth in 2 M NaCl leads to clarification of physiological roles for Kdp and Ktr K+
818 uptake systems. *MBio* **4**.
819 Rahman, M.M., Hunter, H.N., Prova, S., Verma, V., Qamar, A., and Golemi-Kotra, D. (2016) The
820 *Staphylococcus aureus* Methicillin Resistance Factor FmtA Is a d-Amino Esterase That Acts
821 on Teichoic Acids. *MBio* **7**: e02070-02015.
822 Santiago, M., Matano, L.M., Moussa, S.H., Gilmore, M.S., Walker, S., and Meredith, T.C. (2015) A
823 new platform for ultra-high density *Staphylococcus aureus* transposon libraries. *BMC*
824 *Genomics* **16**: 252.
825 Schaefer, K., Matano, L.M., Qiao, Y., Kahne, D., and Walker, S. (2017) In vitro reconstitution
826 demonstrates the cell wall ligase activity of LCP proteins. *Nat Chem Biol* **13**: 396-401.

827 Schindelin, J., Arganda-Carreras, I., Frise, E., Kaynig, V., Longair, M., Pietzsch, T., Preibisch, S.,
828 Rueden, C., Saalfeld, S., Schmid, B., Tinevez, J.Y., White, D.J., Hartenstein, V., Eliceiri, K.,
829 Tomancak, P., and Cardona, A. (2012) Fiji: an open-source platform for biological-image
830 analysis. *Nat Methods* **9**: 676-682.
831 Schuster, C.F., Bellows, L.E., Tosi, T., Campeotto, I., Corrigan, R.M., Freemont, P., and Gründling, A.
832 (2016) The second messenger c-di-AMP inhibits the osmolyte uptake system OpuC in
833 *Staphylococcus aureus*. *Sci Signal* **9**: ra81.
834 Schuster, C.F., and Bertram, R. (2014) Fluorescence based primer extension technique to determine
835 transcriptional starting points and cleavage sites of RNases *in vivo*. *J Vis Exp*: e52134.
836 Schuster, C.F., Howard, S.A., and Gründling, A. (2019) Use of the counter selectable marker PheS*
837 for genome engineering in *Staphylococcus aureus*. *Microbiology*.
838 Schwan, W.R., Lehmann, L., and McCormick, J. (2006) Transcriptional activation of the
839 *Staphylococcus aureus* putP gene by low-proline-high osmotic conditions and during
840 infection of murine and human tissues. *Infect Immun* **74**: 399-409.
841 Scybert, S., Pechous, R., Sitthisak, S., Nadakavukaren, M.J., Wilkinson, B.J., and Jayaswal, R.K. (2003)
842 NaCl-sensitive mutant of *Staphylococcus aureus* has a Tn917-lacZ insertion in its ars operon.
843 *FEMS Microbiol Lett* **222**: 171-176.
844 Sleator, R.D., and Hill, C. (2002) Bacterial osmoadaptation: the role of osmolytes in bacterial stress
845 and virulence. *FEMS Microbiol Rev* **26**: 49-71.
846 Stapleton, M.R., Horsburgh, M.J., Hayhurst, E.J., Wright, L., Jonsson, I.M., Tarkowski, A., Kokai-Kun,
847 J.F., Mond, J.J., and Foster, S.J. (2007) Characterization of IsaA and SceD, two putative lytic
848 transglycosylases of *Staphylococcus aureus*. *J Bacteriol* **189**: 7316-7325.
849 Tong, S.Y., Davis, J.S., Eichenberger, E., Holland, T.L., and Fowler, V.G., Jr. (2015) *Staphylococcus*
850 *aureus* infections: epidemiology, pathophysiology, clinical manifestations, and
851 management. *Clin Microbiol Rev* **28**: 603-661.
852 Townsend, D.E., and Wilkinson, B.J. (1992) Proline transport in *Staphylococcus aureus*: a high-
853 affinity system and a low-affinity system involved in osmoregulation. *J Bacteriol* **174**: 2702-
854 2710.
855 Vaish, M., Price-Whelan, A., Reyes-Robles, T., Liu, J., Jereen, A., Christie, S., Alonzo, F., 3rd, Benson,
856 M.A., Torres, V.J., and Krulwich, T.A. (2018) Roles of *Staphylococcus aureus* Mnh1 and Mnh2
857 Antiporters in Salt Tolerance, Alkali Tolerance, and Pathogenesis. *J Bacteriol* **200**.
858 van den Berg, J., Boersma, A.J., and Poolman, B. (2017) Microorganisms maintain crowding
859 homeostasis. *Nat Rev Microbiol* **15**: 309-318.
860 Vijaranakul, U., Nadakavukaren, M.J., de Jonge, B.L., Wilkinson, B.J., and Jayaswal, R.K. (1995)
861 Increased cell size and shortened peptidoglycan interpeptide bridge of NaCl-stressed
862 *Staphylococcus aureus* and their reversal by glycine betaine. *J Bacteriol* **177**: 5116-5121.
863 Vijaranakul, U., Xiong, A., Lockwood, K., and Jayaswal, R.K. (1998) Cloning and nucleotide
864 sequencing of a *Staphylococcus aureus* gene encoding a branched-chain-amino-acid
865 transporter. *Appl Environ Microbiol* **64**: 763-767.
866 Vollmer, W., Blanot, D., and de Pedro, M.A. (2008) Peptidoglycan structure and architecture. *FEMS*
867 *Microbiol Rev* **32**: 149-167.
868 Wengender, P.A., and Miller, K.J. (1995) Identification of a PutP proline permease gene homolog
869 from *Staphylococcus aureus* by expression cloning of the high-affinity proline transport
870 system in Escherichia coli. *Appl Environ Microbiol* **61**: 252-259.
871 Wertheim, H.F., Melles, D.C., Vos, M.C., van Leeuwen, W., van Belkum, A., Verbrugh, H.A., and
872 Nouwen, J.L. (2005) The role of nasal carriage in *Staphylococcus aureus* infections. *Lancet*
873 *Infect Dis* **5**: 751-762.

874 Wetzel, K.J., Bjorge, D., and Schwan, W.R. (2011) Mutational and transcriptional analyses of the
875 *Staphylococcus aureus* low-affinity proline transporter OpuD during *in vitro* growth and
876 infection of murine tissues. *FEMS Immunol Med Microbiol* **61**: 346-355.
877 Whatmore, A.M., and Reed, R.H. (1990) Determination of turgor pressure in Bacillus subtilis: a
878 possible role for K+ in turgor regulation. *J Gen Microbiol* **136**: 2521-2526.
879 Wood, J.M. (2011) Bacterial osmoregulation: a paradigm for the study of cellular homeostasis. *Annu*
880 *Rev Microbiol* **65**: 215-238.
881 Wyke, A.W. (1984) Isolation of five penicillin-binding proteins from *Staphylococcus aureus*. *FEMS*
882 *Microbiology Letters* **22**: 133-138.
883 Yao, J., Zhong, J., Fang, Y., Geisinger, E., Novick, R.P., and Lambowitz, A.M. (2006) Use of targetrons
884 to disrupt essential and nonessential genes in *Staphylococcus aureus* reveals temperature
885 sensitivity of Ll.LtrB group II intron splicing. *RNA* **12**: 1271-1281.
886 Zeden, M.S., Schuster, C.F., Bowman, L., Zhong, Q., Williams, H.D., and Gründling, A. (2018) Cyclic
887 di-adenosine monophosphate (c-di-AMP) is required for osmotic regulation in
888 *Staphylococcus aureus* but dispensable for viability in anaerobic conditions. *J Biol Chem* **293**:
889 3180-3200.
890

891

892 **Figure legends**

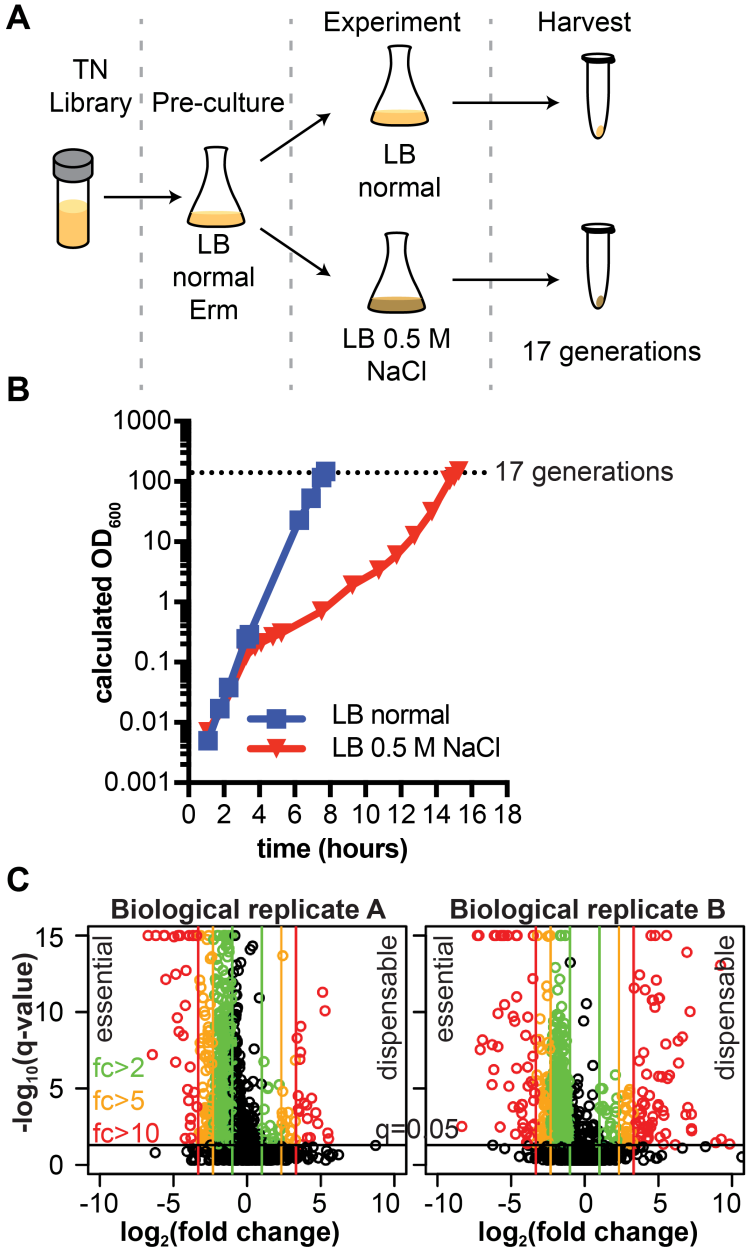

893

894 **Fig. 1. TN-Seq screen reveals essential and dispensable genes during prolonged NaCl stress in *S.***
895 ***aureus*.**

896 A. Workflow of TN-seq experiments. A saturated transposon library was pre-cultured for one hour,
897 then used to inoculate LB medium containing either normal levels (0.086 M) or 0.5 M of NaCl. After
898 17 generations, cells were harvested, and transposon insertion sites determined by high throughput
899 sequencing.

900 B. Growth curve. Growth of the *S. aureus* library culture in LBN and LB 0.5 M medium was followed
901 by determining OD_{600} readings. Dotted line indicates the 17 generation threshold. Cultures were

902 back-diluted once when they reached an OD of approximately 0.3 and the optical densities shown
903 are calculated from measured ODs time dilution factor. Culture from replicate B (n=1) is shown and
904 a similar growth profile was seen for replicate A.
905 C. Volcano plots of essential and dispensable genes in NaCl conditions compared to LBN. Negative
906 log_2 fold-changes indicate essential and positive log_2 fold-changes dispensable genes. q-value stands
907 for Benjamini-Hochberg false discovery rate. Black horizontal line indicates q-value of 0.05 (cut-off)
908 and red, orange and green vertical lines 10-, 5- and 2-fold differences in either direction. Colored
909 circles indicate genes for which a significant change in the number of transposon insertions was
910 observed above q-value cutoff and follow the same color code as the vertical lines. Very small q-
911 values were truncated to fit onto the graph. Data from replicate A are shown in the left panel and
912 from replicate B in the right panel (n=1 for each plot).

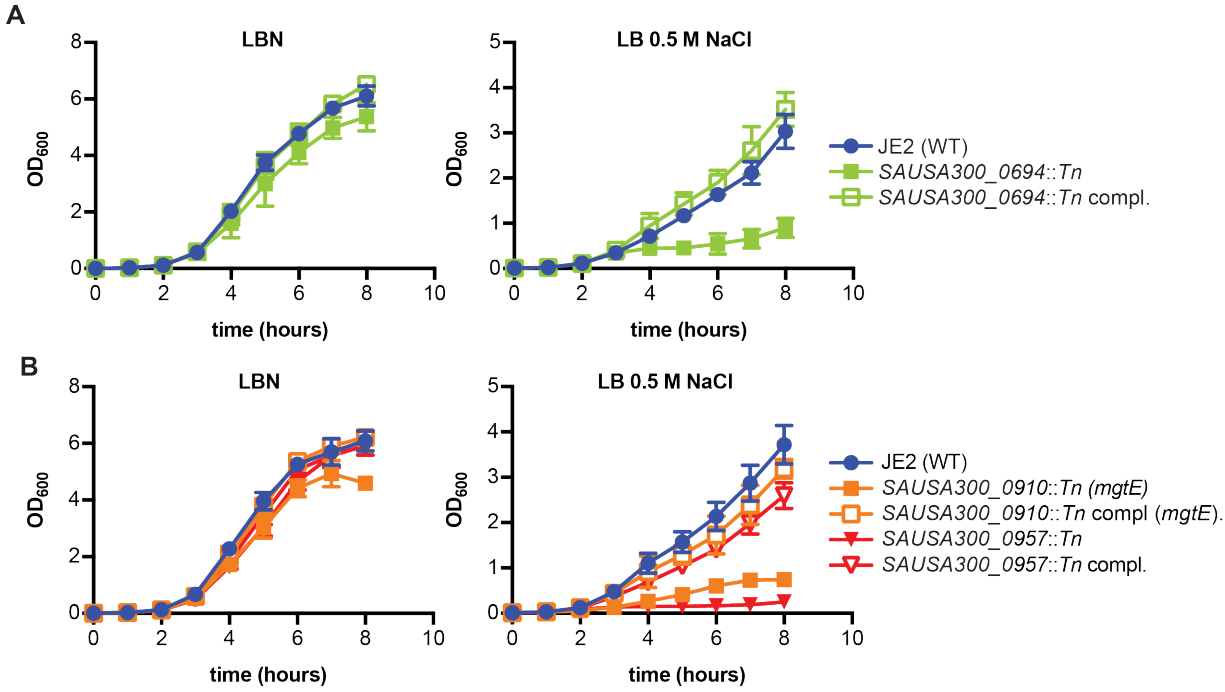

Fig. 2. Growth curves and complementation analysis of *S. aureus* strains with transposon insertions in salt essential genes.

A-B. *S. aureus* strains JE2 (WT), *SAUSA300_0694::Tn* mutant with empty plasmid and complementation strain (A) or JE2 (WT), *SAUSA300_0910* (*mgtE*), *SAUSA300_0957::Tn* with empty plasmid (B) and respective complementation strains were grown in LBN (left panels) or LB 0.5 M NaCl medium (right panels) supplemented with 100 ng/ml Atet and OD_{600} readings determined at timed intervals. Growth curves were performed in triplicates (n=3) and means and SDs of OD_{600} readings were plotted.

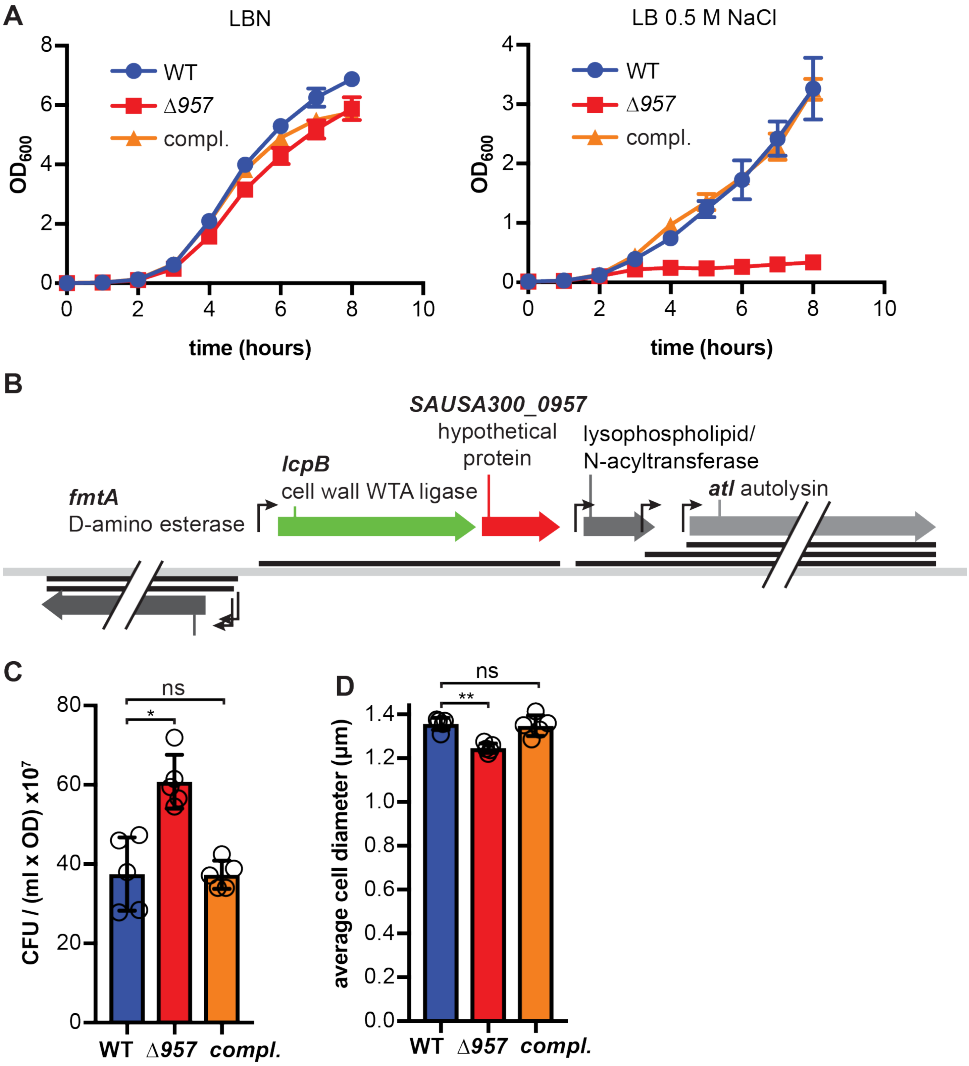

Fig. 3. Gene *SAUSA300_0957* is located in a genomic region with cell envelope genes and its deletion leads to salt sensitivity and other phenotypic changes.

A. Growth curves. *S. aureus* strains LAC* piTET (WT), LAC*Δ*957* piTET (Δ*957*) and the complementation strain LAC*Δ*957* piTET-*957* (compl.) were grown in LBN or LB containing 0.5 M NaCl medium and 100 ng/ml Atet. The growth was monitored by determining OD_{600} readings the means and SDs from three independent experiments were plotted.

B. Schematic of the *S. aureus* USA300 FPR3757 chromosomal region with gene *SAUSA300_0957* (gene *957*). Putative promoters are shown as angled arrows (adapted from (Mäder *et al.*, 2016)) and black bars indicate the corresponding transcripts.

934 C. Determination of CFU/OD ratios. OD_{600} values as well as CFU/ml were determined for overnight
935 cultures of the *S. aureus* strains described in panel B and the means and SDs of the CFU per ml OD_{600}
936 of 1 from five independent experiments were plotted.
937 D. Cell size measurements. The cell walls of the *S. aureus* strains described in panel B were stained
938 with fluorescently labelled vancomycin and the cells subsequently observed under a microscope.
939 The diameters of 200 cells were measured and the means calculated. This average of the means and
940 SDs from five independent experiments were plotted.
941 For statistical analysis, a Kruskal-Wallis one-way ANOVA test was performed followed by a Dunn's
942 post-hoc test to determine p-values. Asterisks (*) indicate $p \leq 0.05$ and two asterisks (**) $p \leq 0.01$ and
943 ns=not significant.
944

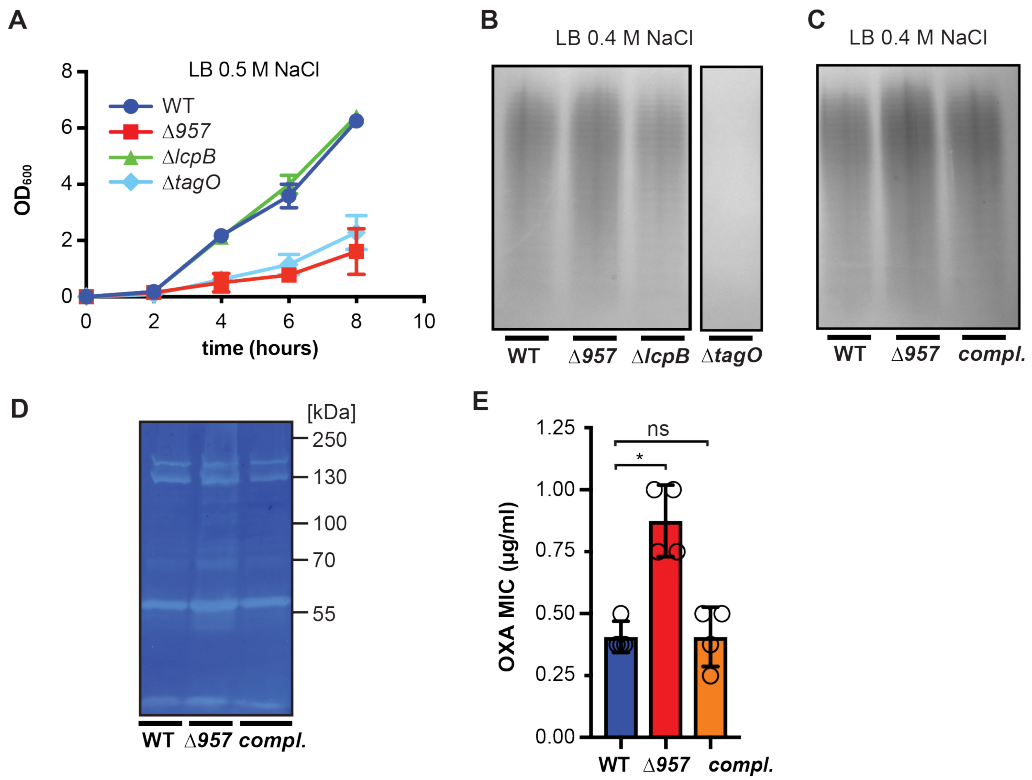

Fig. 4. Inactivation of *gene 957* does not significantly alter WTA levels or autolysis but leads to changes in oxacillin resistance

A. Growth curves. *S. aureus* strains LAC* (WT), LAC*Δ*957* (Δ*957*), LAC*Δ*lcpB*, (Δ*957*), and LAC*Δ*tagO* (Δ*tagO*) were grown in LB 0.5 M NaCl medium and OD_{600} readings determined at timed intervals. The means and SDs from three biological replicates were plotted.

B. Detection of WTA on silver stained gels. WTA was isolated from *S. aureus* strains described in panel A following growth in LB 0.4 M NaCl medium. The WTA was separated by electrophoresis and visualized by silver stain. The experiment was performed three times and one representative gel image is shown.

C. Detection of WTA on silver stained gels. Same as panel B but using the strains LAC* piTET (WT), LAC*Δ*957* piTET (Δ*957*), and the complementation strain LAC*Δ*957* piTET-*957* (compl.) grown in LB 0.4 M NaCl medium also containing 100 ng/ml Atet.

D. Zymogram gel. Cell extracts prepared from *S. aureus* strains described in panel C were separated on a gel containing heat killed *Micrococcus luteus* cells. Autolysins were renatured and the zones of

960 lysis visualized by methylene blue staining. The experiment was performed twice and one
961 experiment is shown.
962 E. Determination of oxacillin MICs. Oxacillin MICs were determined for *S. aureus* strains described
963 in panel C using Etest strips. The median and SDs from four biological replicates were plotted.
964 For statistical analysis, a Kruskal-Wallis one-way ANOVA test was performed followed by a Dunn's
965 post-hoc test to determine p-values. Asterisks (*) indicate $p \leq 0.05$ and ns=not significant.
966

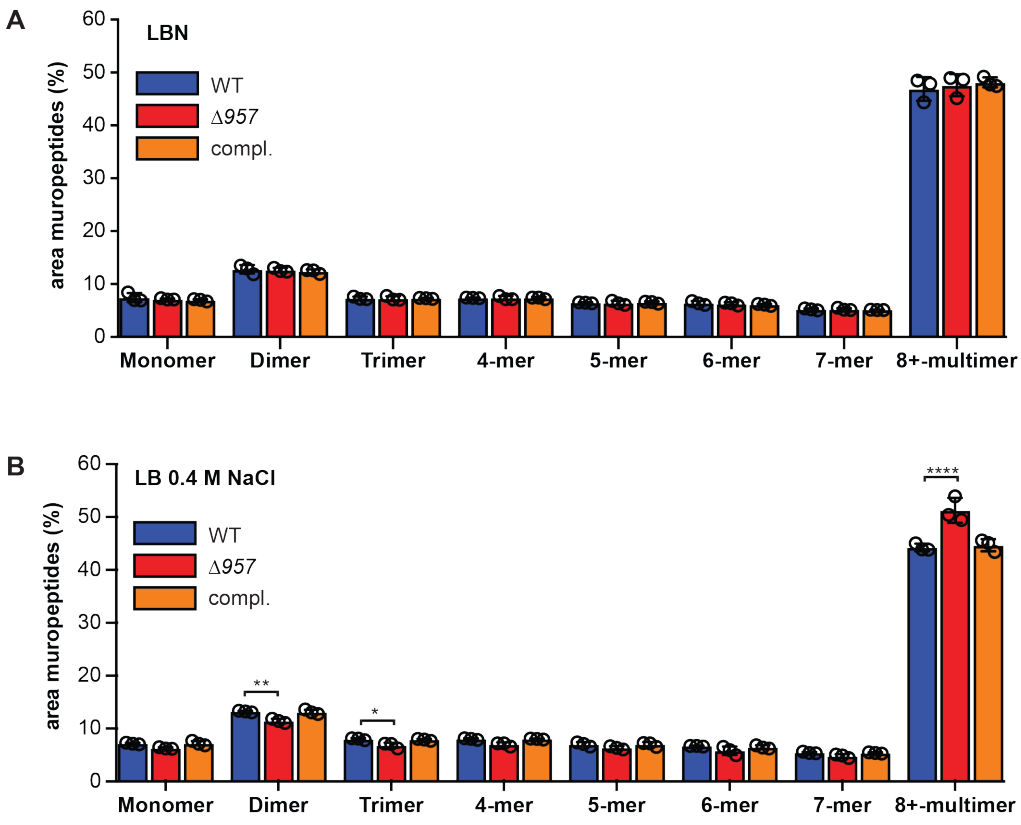

967

968 **Fig. 5. Inactivation of *gene 957* leads to an increase in peptidoglycan crosslinking.**

969 A-B. Muropeptide quantification. *S. aureus* strains LAC* piTET (WT), LAC*Δ*957* piTET (Δ*957*), and
970 the complementation strain LAC*Δ*957* piTET-*957* (compl.) were grown in either LBN (A) or LB 0.4 M
971 NaCl (B) containing 100 ng/ml Atet. After reaching late-exponential phase, the peptidoglycan was
972 isolated, digested and the muropeptides separated by HPLC. The areas under the peaks from the
973 chromatograms (representative chromatograms are shown in Supplementary Fig. S5) were
974 quantified for each mono-, di- or multimer. Bars represent means, and error bars standard
975 deviations from three independent experiments. For statistical analyses, two-way ANOVAs were
976 performed, followed by Dunnett's post-hoc tests using the WT as a comparison. The differences in
977 (A) were not significant. For (B), one asterisk (*) indicates $p \leq 0.05$, two asterisks (**) $p \leq 0.01$ and four
978 asterisks (****) $p \leq 0.0001$.

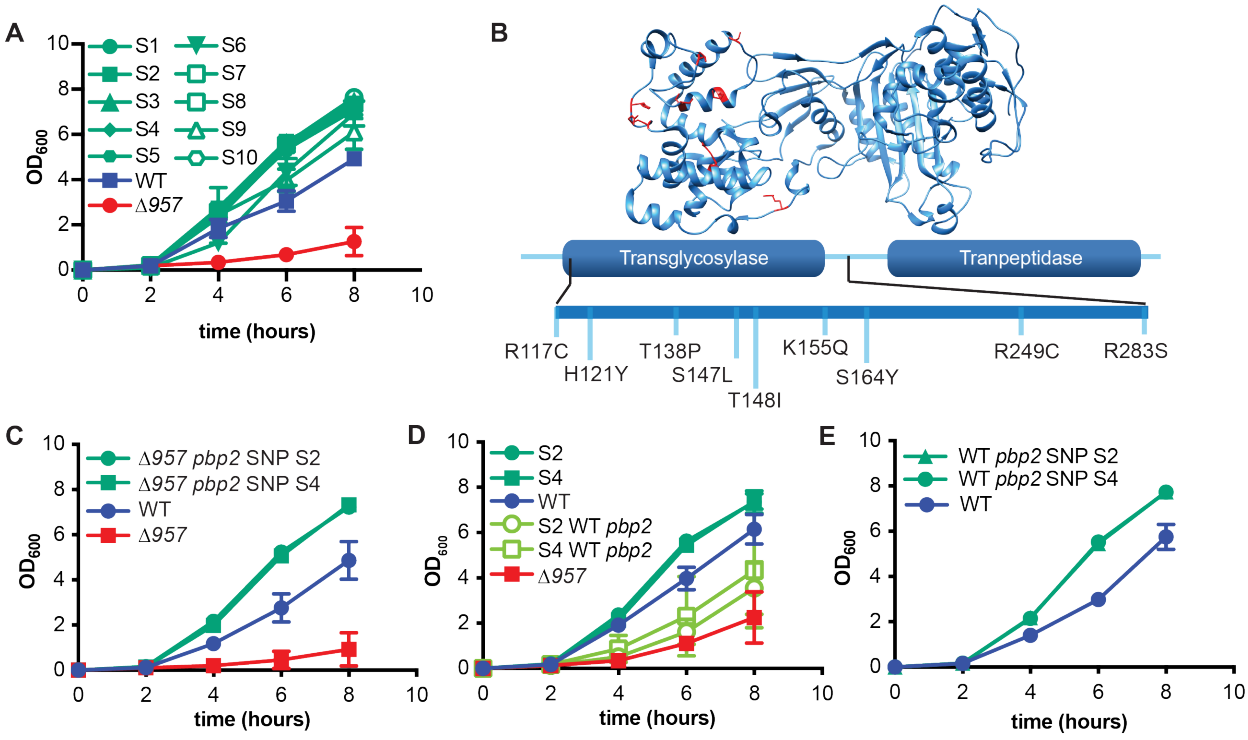

Fig. 6. The growth and peptidoglycan defect observed for the *957* mutant can be rescued by compensatory mutations in *pbp2*.

A. Growth curves. *S. aureus* strains LAC* (WT), LAC*Δ*957* (Δ*957*) and the LAC*Δ*957* suppressors S1-10 (S1 to 10) were grown in LB 0.5 M NaCl medium, OD_{600} readings determined and the means and SDs of four biological replicates plotted.

B. Schematic of Pbp2 with amino acid substitutions identified. Top: Structure of the *S. aureus* penicillin binding protein Pbp2 (PDB: 3DWK, (Lovering *et al.*, 2008)) with amino acids that are altered in the obtained suppressor strains shown in red. Bottom: Schematic of the Pbp2 enzyme with the transglycosylase and transpeptidase domains as well as the observed amino acid changes in the transglycosylase domain indicated.

C. Growth curves using *957* mutant strains containing *pbp2* alleles from suppressors S2 and S4. Growth curves were performed in LB 0.5 M NaCl medium and plotted as described in panel A but

992 using *S. aureus* strains LAC* *1332*::Tn (WT), LAC*Δ*957* *1332*::Tn (Δ*957*), LAC*Δ*957* *1332*::Tn *pbp2*

993 SNP S2 (Δ*957* *pbp2* SNP S2), LAC*Δ*957* suppressor S4 *1332*::Tn (Δ*957* *pbp2* SNP S4).

994 D. Growth curves using *957* suppressors with their *pbp2* gene repaired to WT. Growth curves were

995 performed in LB 0.5 M NaCl medium and plotted as described in panel A but using *S. aureus* strains

996 LAC* *1332*::Tn (WT), LAC*Δ*957* *1332*::Tn (Δ*957*), LAC*Δ*957* suppressor S2 *1332*::Tn (S2), LAC*Δ*957*

997 suppressor S4 *1332*::Tn (S4), LAC*Δ*957* suppressor S2 *1332*::Tn repaired WT *pbp2* (S2 WT *pbp2*),

998 and LAC*Δ*957* suppressor S4 *1332*::Tn repaired WT *pbp2* (S4 WT *pbp2*).

999 E. Growth curves using WT strains carrying *pbp2* SNPs. *S. aureus* strains LAC* *1332*::Tn (WT), LAC*

1000 *1332*::Tn *pbp2* SNP S2 (WT *pbp2* SNP S2) and LAC* *1332*::Tn *pbp2* SNP S4 (WT *pbp2* SNP S4) were

1001 grown in LB 0.5 M NaCl medium and OD_{600} readings determined and the means and SDs of three

1002 biological replicates plotted.

1003

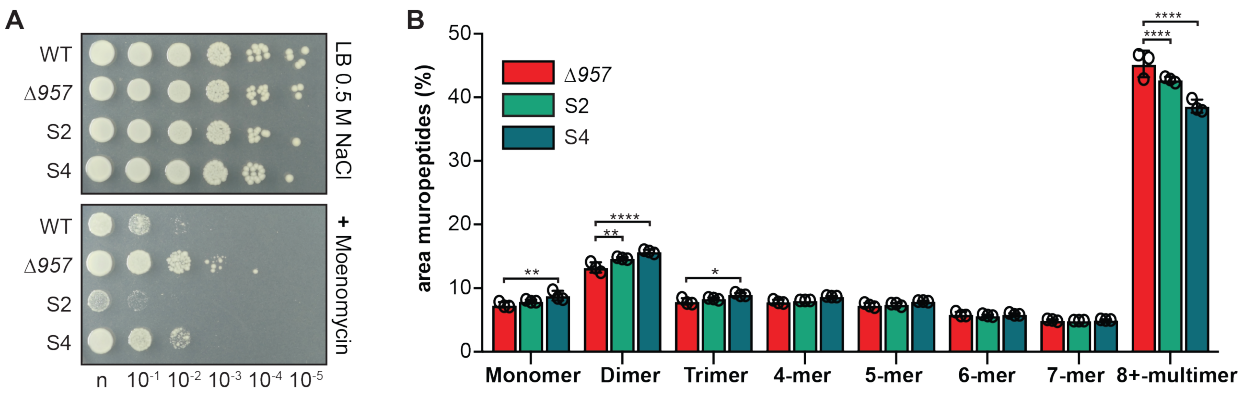

Fig. 7. The Δ*957* suppressor strains show decreased peptidoglycan crosslinking compared the Δ*957* mutant.

A. Bacterial growth on moenomycin supplemented agar plates. *S. aureus* strains LAC* (WT), LAC*Δ*957* (Δ*957*), LAC*Δ*957* Suppressor S2 (S2) and S4 LAC*Δ*957* Suppressor S4 (S4) were grown to exponential phase, normalized to an OD_{600} of 0.1 and plated either neat (n) or in 10-fold dilutions onto LB agar containing 0.5 M NaCl without (top) or with (bottom) moenomycin. Shown is one representative image of three biological replicates.

B. Muropeptide analysis. *S. aureus* strains LAC*Δ*957* (Δ*957*), LAC*Δ*957* Suppressor S2 (S2) and S4 LAC*Δ*957* Suppressor S4 (S4) were grown in 0.4 M NaCl LB medium and muropeptides quantified as described in Fig. 5. Representative chromatograms are shown in Supplementary Fig. S6D. The means and SDs from three biological replicates were plotted. For statistical analysis a two-way ANOVA and Dunnett's post-hoc test was performed. One asterisk (*) indicates $p \leq 0.05$, two asterisks (**) $p \leq 0.01$ and four asterisks (****) $p \leq 0.0001$.